Journal of Membrane Science 708 (2024) 123054

Contents lists available at ScienceDirect

Journal of Membrane Science

journal homepage: www.elsevier.com/locate/memsci

Fractionation and refining of pectic oligosaccharides derived from onion skins through continuous feed diafiltration

M.O. Ruiz *, Ó. Benito-Román, S. Beltrán, M.T. Sanz

Department of Biotechnology and Food Science, Chemical Engineering Division, University of Burgos, Plaza Misael Bañuelos s/n 09001, Burgos, Spain

ARTICLE INFO

Keywords:
Pectic oligosaccharide fractionation
Diafiltration purification
Membrane fouling
Onion skin byproduct
Green technologies

ABSTRACT

In this work, a diafiltration-based process was investigated for the recovery of pectic oligosaccharides produced by subcritical water hydrolysis from onion skin waste. Four tubular ceramic membranes from 100 to 1 kDa were selected based on the molecular weight of the different galacturonic acid species present in the onion skin hydrolysate. All these membranes showed high selectivity towards pectic oligosaccharides, with low retention for free galacturonic acid, monosaccharides, organic acids, and other impurities. The 50 and 100 kDa membranes completely retained pectic oligosaccharides with a molecular weight exceeding 80 kDa, accounting for approximately 30 % of the initial pectic oligosaccharides in the hydrolysate. However, the purification rate was significantly slower using the 50 kDa membrane due to the increased cake layer resistance. Furthermore, it was examined a fractionation/purification cascade involving sequential diafiltration stages using 100, 10, and 1 kDa membranes at 25 °C, TMP = 1 bar, and a crossflow velocity of 1.5 m s^{-1}. Approximately 87 % of the initial pectic oligosaccharides were successfully recovered and purified in the retentates, highlighting their potential for diverse applications due to their narrow molecular weight distribution, while phenolic compounds and other valuable low molecular weight molecules were recovered in the final permeate.

1. Introduction

Onion processing yields large amounts of skin residues, which are characterized by its high environmental impact and the presence of valuable bioactive compounds [1], such as quercetins and derivatives [2,3]. Furthermore, the solid waste after the extraction of these phenolic compounds is a promising natural source of pectin [1,3] from which pectic oligosaccharides (POS) can be produced. These pectin-derived oligosaccharides, rich in 1,4-D-galacturonic acid and neutral sugars (commonly rhamnose, galactose, arabinose, and xylose), find application as functional agents in the realms of food, healthcare, and pharmaceuticals due to their capacity to modulate the microbiota within the human intestine and their anti-inflammatory and anti-obesity properties [4–7].

The conventional process for producing POS typically involves partial acid or enzymatic hydrolysis of pectin [5]. However, subcritical water extraction offers notable potential in this regard, as it has previously been proposed as an environmentally friendly reaction medium for obtaining different chemical compounds from solid by-products [8–11]. Subcritical water refers to water at temperatures ranging from 100 °C to 374 °C (critical point), which remains in a liquid state due to the application of pressure. As a consequence of the higher ionic strength and lower pH of subcritical water, pectin can be extracted from the solid matrix and hydrolysed without the necessity of adding acids, enzymes, or organic solvents [12,13]. Benito-Román et al. [14] have previously found that pectin extracted and hydrolysed from onion skin waste using a subcritical water at 145 °C for 50 min preserves the branched domains of ramnogalacturonan- I (RG-I) in the resulting pectin oligomers. These RG-I domains comprise numerous side chains formed by neutral sugars [15], which can enhance the nutritional and pharmaceutical value of POS. However, in practice, a separation process is required to isolate these valuable pectic oligosaccharides from subcritical water hydrolysates. Monosaccharides, organic acids, and sugar dehydration products (furfural and HMF) have been identified as the main impurities in the hydrolysates derived from pectin-rich solid residues [14–16]. Currently, precipitation is employed as purification process, accomplished through the addition of ethanol (a salting-out process) and followed by subsequent steps involving dialysis, ionic exchange, nitration, or combinations thereof [17,18]. Nevertheless, the use of ethanol raises environmental concerns and lacks selectivity [4,

* Corresponding author.
E-mail address: moruiz@ubu.es (M.O. Ruiz).

https://doi.org/10.1016/j.memsci.2024.123054
Received 22 May 2024; Received in revised form 30 June 2024; Accepted 2 July 2024
Available online 3 July 2024

19], often resulting in monosaccharides and POS remaining in the alcohol solution [7]. Therefore, there is a compelling need for efficient tools that enable an effective and cost-efficient separation of the complex product obtained.

For this purpose, ultrafiltration (UF)-based diafiltration process emerges as a cost-effective alternative to the traditional precipitation method for separating POS. This approach offers several advantages, including ease of automation and scalability, minimal energy consumption, absence of organic solvents or other precipitating agents, under mild operation conditions [20,21]. Diafiltration processes rely on the separation of molecules in solution due to their different rejection rates by the membrane. A diluent, typically water, is intermittently or continuously pumped into the feed side to facilitate the transport of molecules with lower rejection rates, which generally correspond to the smallest molecular weight species for ultrafiltration membranes [22–24]. In fact, ultrafiltration in diafiltration mode employing organic membranes ranging from 1 to 100 kDa has been investigated as a potential POS purification process. For instance, ultrafiltration in intermittent feed diafiltration mode was employed to process a subcritical water hydrolysate from lemon peel waste using a 1 kDa regenerated cellulose membrane, achieving notably high purities (up to 98 g oligomers per 100 g dry product) as reported Gómez et al. [15]. However, in a different study by Yammine et al. [25], the purification of POS from a grape pomace subcritical water hydrolysate necessitated a cascade of continuous feed diafiltration stages, utilising organic membranes with cutoff sizes of 100, 50, and 2 kDa. Pinelo et al. [26] have already reported that the degree of linearity or branching of pectinaceous substances greatly affects their ability to pass through the membrane pores. In this context, a proper assessment of the molecular weight cutoff (MWCO) of the membrane is required to achieve efficient fractionation and purification of the POS species. It is also important to note that challenges related to diafiltration productivity, such as water consumption and membrane fouling, are often overlooked when dealing with these types of oligosaccharides.

Ceramic membranes are emerging as a promising alternative to organic membranes due to their exceptional separation accuracy, chemical stability across a wide pH and temperature range, high resistance to wear, extended lifespan, and ease of cleaning [27–30]. The complex chemical composition and acidic pH of onion skin waste subcritical water hydrolysates make ceramic membranes the preferred choice for the development of POS separation processes. However, it should be indicated that severe fouling of ceramic membranes has been detected in the separation of pectin and derivatives from model solutions, wastewater, and natural juices [26,31–33].

This study aims to assess the feasibility of crossflow ultrafiltration in diafiltration mode using TiO_2 membranes to fractionate and purify the pectic oligosaccharides present in onion skin waste subcritical water hydrolysates. In the existing literature, it is hard to find examples showing the fractionation of pectin-derived oligosaccharides through sustainable membrane technology, particularly employing diafiltration processes with ceramic membranes. Therefore, a comprehensive investigation in total recirculation is necessary to examine the impact of membrane cutoff size on separation efficiency of the different main hydrolysate compounds. Furthermore, it is essential to delve into the fouling mechanisms, given that continuous feed diafiltration is a complex kinetic purification process demanding modelling for its successful scaling-up towards industrial implementation. The last objective of this work was to assess the overall efficiency of a series of diafiltration stages utilising membranes with varying molecular weight cutoff sizes. This aims to generate multiple high-purity POS fractions with differing molecular weights, thereby offering versatile functional additives for industrial applications.

2. Experimental

2.1. Chemicals and materials

Onion (*Allium cepa*) skin residues corresponded to the cultivar Horcal and were kindly provided by a local blood sausages manufacturer (Embutidos Cardeña, Burgos, Spain). The 1–100 kDa cutoff-sized tubular ceramic membranes (Filtanium, with an active layer of TiO_2 supported on titania) were supplied by TAMI industries (France). The TAMI membranes consisted of a single tubular module (254 mm length, 10 mm outside diameter) with 7 inner channels (2 mm hydraulic diameter), an isoelectric point close to 4.2 [34] and an effective filtration area of 0.0132 m^2. Glucose (99.5 %), galactose (99 %), arabinose (99 %), rhamnose (99 %), xylose (99 %), D-glucuronic acid (98 %), acetonitrile (99.9 %), and furfural (99 %) were supplied by Sigma-Aldrich (USA). 5-hydroxymethyl furfural (97 %) was provided from Biosynth Ltd. (United Kingdom); D-galacturonic acid monohydrate (purity >97 %) was obtained from Alfa Aesar (USA). Formic acid (98 %) and acetic acid glacial (99.7 %) were purchased from Panreac (Spain); orthophosphoric acid (76 %) and sodium hydroxide (99 %) from Cofarcas S.A. (Spain), and ammonium acetate (LiChropur™, ≥99 %) form Merck (Germany). Sulfuric acid used for the sample hydrolysis was 96 % purity and was provided by Labbox (Spain), whereas the one used for the HPLC mobile phase preparation was 96 % Suprapur provided by Merck (Germany). All chemicals were used without further purification.

2.2. Biomass preparation

Industrial onion skin residues (IOSR) underwent manual processing to isolate the outermost skins, which were subsequently air-dried at room temperature. The dried material was further reduced in size to particles smaller than 1 mm using a Retsch SM100 cutting mill (Retsch GmbH, Germany), to a particle size of less than 1 mm, ensuring suitability for suspension within the reactor. The dried solid was then subjected to an extraction process with an ethanol/water mixture (70/30 v/v%) at 37 °C in order to recover the primary portion of the phenolic fraction (~10 % of biomass extractive content), following the procedure established by Benito-Román et al. [14]. The solid waste from the IOSR, obtained after the recovery of primary phenolic compounds, was subsequently dried once more and employed as pectin biomass for the subcritical water hydrolysis experiments.

2.3. Hydrolysate preparation from onion skin waste

Subcritical water (SubW) hydrolysis experiments were carried out using a discontinuous system, consisting of a 0.5 L batch reactor coupled with a ceramic electric band heater (2000 W, manufactured by SAF Wärmetechnik GmbH, Germany) and nitrogen as pressurizing agent. The reactor maximum specifications were 250 °C and 70 bar. The SubW treatment was carried out at 145 °C and 50 bar for 50 min with a biomass concentration of 4.3 % (w/v). The solid residue and water were first loaded in the reactor, then the system was heated and stirred continuously using a magnetic stirrer (Agimatc-E, J.P.-Selecta, Spain) placed under the reactor. Subsequently, the system was pressurized to achieve the desired working pressure. After the SubW hydrolysis was finished, the reactor was cooled down to 90 °C. Subsequently, it was opened, and the suspension was filtered using cheesecloth (Thermo Fisher Scientific Inc., United Kingdom). The exhausted onion skin biomass was discarded and the liquid phase (named onion skin hydrolysate, OSH) was centrifuged (model SorVall™ ST16R, Thermo Scientific, MA-USA), characterized in terms of composition and frozen at −20 °C. This OSH was used as feed solution in all ultrafiltration assays.

2.4. Crossflow ultrafiltration experiments

2.4.1. Filtrations in total recirculation mode

Experiments in total recirculation mode were carried out using the experimental setup depicted in Fig. 1A. The feed hydrolysate was pumped from a stirred feed tank (Pobel, Spain) to the membrane module by means of a Masterflex peristaltic pump (HV-7220-57 equipped with a Masterflex L/S EasyLoad II head HV-77201-62, Masterflex SE, Germany), using silicone pipes (Masterflex L/S 15, 4.8 mm internal diameter, Masterflex SE, Germany). Two pressure gauges measured the pressures at the inlet and outlet of the membrane module. The crossflow velocity (CFV) and the transmembrane pressure (TMP) were adjusted to the desired working value using the pump speed controller (from 6 to 600 rpm) and a valve placed downstream the membrane module. All experiments were carried out at a constant temperature of 25 °C and CFV of 1.5 ± 0.1 m s^{-1} (feed flow rate of 17.5 L h^{-1}) by recycling permeate and retentate continuously to the feed tank in order to maintain a constant feed concentration during membrane filtration. This crossflow velocity was the maximum value to avoid problems in the pressure drop along the membrane unit caused by foaming during OSH

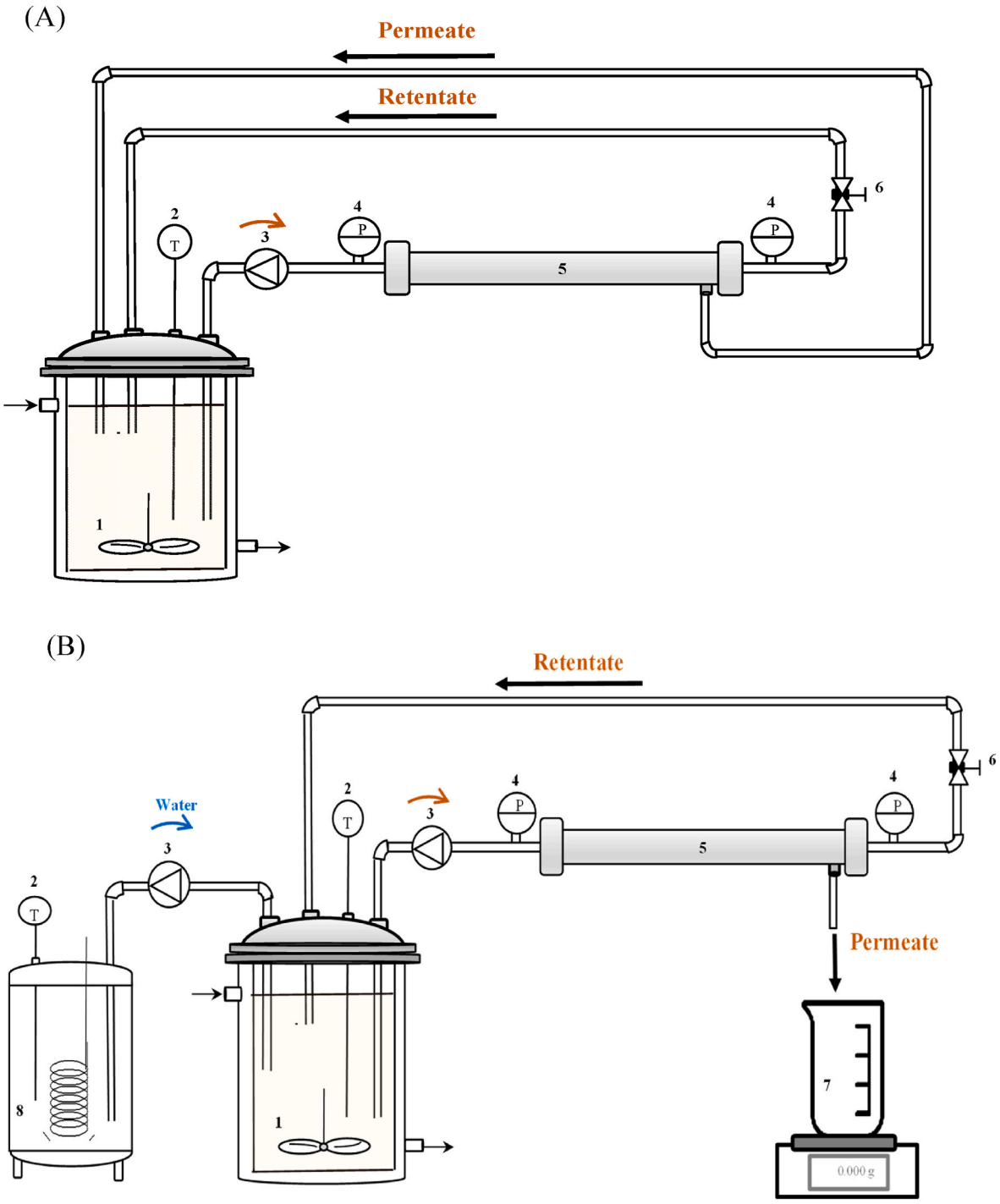

Fig. 1. Schematic diagram of the experimental setup for ultrafiltration experiments (A) in total recirculation mode and (B) in continuous feed diafiltration mode. 1. Feed jacked tank; 2. Thermometer; 3. Peristaltic pump; 4. Pressure gauge; 5. Tubular membrane module; 6. Regulating recirculation valve 7. Permeate vessel; 8. Water tank.

filtration. The temperature was set at 25 °C in order to avoid heating of the onion skin hydrolysate, minimise the energy cost, and to assess the feasibility of the ultrafiltration process at ambient temperature. Permeate fluxes (J) were determined volumetrically (±0.1 mL) and gravimetrically (±0.001 g) at different operating conditions including MWCO (1–100 kDa) and TMP (0.25–1.5 bar). After 120 min of filtration, samples were collected from the retentate and permeate sides to measure the separation performance.

2.4.2. Filtrations in diafiltration mode

The continuous feed diafiltration (CFD) experiments were carried out using the experimental setup shown in Fig. 1B. The onion skin hydrolysate was placed in a stirred feed tank (Pobel) and pumped to the membrane module by means of a Masterflex peristaltic pump (HV-7220-57 with a Masterflex L/S EasyLoad II head HV-77201-62, Masterflex SE, Germany). Another Masterflex peristaltic pump (HV-7521-10 with a Masterflex L/S EasyLoad II head HV-77200-50, Masterflex SE, Germany) was used to add deionised water to the feed tank. The pipes were silicone tubing (Materflex L/S 15, Masterflex SE, Germany). Two pressure gauges measured the pressures at the inlet and outlet of the membrane module. Before starting the filtration process, the feed solution was recirculated through the system for 5 min. Then, TMP and CFV were adjusted to the desired working value using the pump speed controller and a valve placed downstream the membrane module.

The diafiltration experiments were carried out at constant TMP = 1.00 ± 0.05 bar, CFV = 1.5 ± 0.1 m s^{-1} (feed flow rate of 17.5 L h^{-1}) and 25 °C by continuously withdrawing the permeate. The retentate was recycled back to the feed tank, the permeate was collected in the permeate tank, while water was added to the feed tank at a flow rate equal to the permeate outflow rate ($V_p = V_w$) in order to keep the volume in the feed tank constant (V_F=V_r). Permeate fluxes were measured volumetrically (±0.1 mL) and gravimetrically (±0.001 g) until the end of the experiment. The diafiltration volume (water consumption), DV, was calculated as the ratio of the volume of water added in the feed tank to the constant retentate volume (DV=V_w/V_r). The permeate and the retentate were periodically analysed and the concentration of different hydrolysate compounds was represented against the DV ratio in order to evaluate the mass transfer rate, the membrane fouling and separation degree.

2.4.3. Experiments with sequential diafiltration stages

The flowchart of the POS fractionation cascades is shown in Fig. 2. Filtration experiments were carried out using the 1, 10 and 100 kDa membranes. Two independent cycles of sequential ultrafiltration stages were performed in order to determine the membrane separation capacity and POS recovery factors. The feed solution (OSH) was ultrafiltered in diafiltration mode through a 100 kDa membrane, obtaining a first permeate (p1) and retentate (r1). This first permeate p1 from the 100 kDa membrane was then ultrafiltered in diafiltration mode through a 1 kDa membrane (*Cycle A*).

In *Cycle B*, p1 from the 100 kDa membrane was ultrafiltered in concentration mode with a 10 kDa membrane until a volume reduction factor (VRF=V_{p1}/V_{p^*}) of 2.6 was reached, and then, the resulting retentate (r*) and permeate (p*) were subjected to a diafiltration stage through a 10 kDa membrane and a 1 kDa membrane, respectively.

All diafiltration stages and the concentration stage in *Cycle B* were performed at constant TMP of 1.00 ± 0.05 bar, CFV of 1.5 ± 0.1 m s^{-1} and 25.0 ± 0.1 °C by continuously withdrawing the permeate. The retentate was recycled back to the feed tank, the permeate stream was collected in permeate tank throughout the filtration and water was added to the feed tank at the same permeate outflow rate in diafiltration stages. The membrane was not cleaned between the concentration and CFD stages in *Cycle B*, i.e., the process was continuous.

2.4.4. Membrane cleaning procedure

All ceramic membranes were cleaned after each experiment to restore the initial water permeability. The membrane was rinsed with deionised water, and then cleaned with a sodium hydroxide solution (0.2 M, 50 °C and TMP = 0.3 bar) for 60 min. After that, the membrane was rinsed again with deionised water and the water permeate flux was

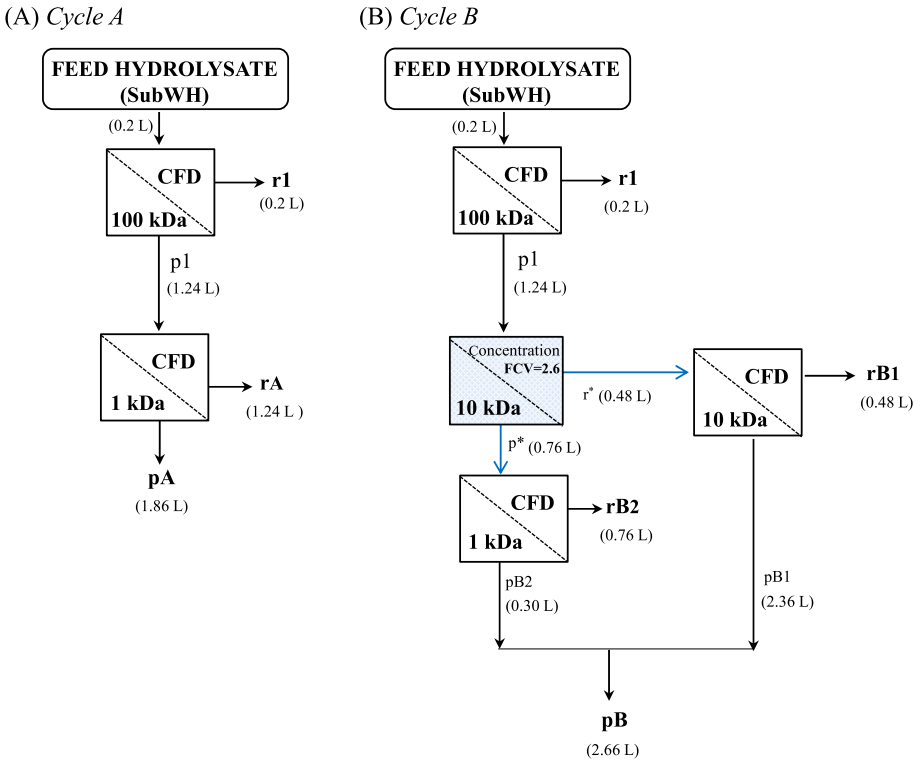

Fig. 2. Flowchart representing the diafiltration cascades for the fractionation and purification of the onion skin pectic oligosaccharides. CFD and Concentration, refer to the ultrafiltration stage in continuous feed diafiltration mode and in concentration mode, respectively.

measured at 25 °C under different transmembrane pressures in order to evaluate the membrane cleaning extent.

2.5. Analytical methods

The feed hydrolysate, along with the permeates and retentates, have been chemically and physically characterised.

Determination of pectic oligosaccharides (POS), free monosaccharides and degradation products. Identification and quantification of sugars, organic acids and sugar dehydration products in the samples was carried out following protocol NREL/TP-510–42623 by high-performance liquid chromatography (HPLC). For that purpose, the HPLC system (Agilent Technologies, CA, USA) equipped with a Biorad Aminex HPX-87 H column (300 × 7.8 mm, Bio-Rad laboratories, Inc., USA) coupled with the guard column Micro-Guards Cation H+ (BioRad laboratories, Inc., USA), with a variable wavelength detector (VWD) and a refractive index detector (RID), using 0.005 M sulfuric acid as mobile phase (0.6 mL/min) was used. The column and detectors were maintained at 40 °C and the total running time was 67 min per injection. The standards for the HPLC analysis were glucose, galactose, xylose, rhamnose, arabinose, 5-hydroxymethyl furfural and furfural, and other compounds such as glucuronic acid, galacturonic acid, acetic acid and formic acid. Free monosaccharides, free galacturonic acid and other compounds in the samples were first determined, after centrifugation (4500 rpm, 15 min, 4 °C) and filtration through a 0.22 μm pore size syringe filter (Scharlab, Spain). Total sugars and total galacturonic acid were determined after acid hydrolysis of the sample according to the NREL/TP-510–42618 Analytical Procedure. POS fraction was calculated as the difference between total galacturonic acid and sugar content after acid hydrolysis and the free galacturonic acid and monosaccharide content. The proportions of homogalacturonan (HG) and rhamnogalacturonan type I (RG-I) have been calculated according to the equations proposed by M'Sakni et al. [35]:

$$\mathrm{HG}\ (\%, \mathrm{mol}) = \mathrm{GAO} - \mathrm{rhaO} \tag{1}$$

$$\mathrm{RG-I}\ (\%, \mathrm{mol}) = [\mathrm{GAO} - \mathrm{HG}] + \mathrm{rhaO} + \mathrm{galO} + \mathrm{xylO} + \mathrm{araO} \tag{2}$$

where GAO, rhaO, galO, xylO and araO refer to the molar percentage of galacturonic acid, rhamnose, galactose, xylose, and arabinose in oligomeric form.

Molecular weight analysis for POS fractions. The molecular weight (MW) distribution, average molecular weights and polydispersity of the pectic oligosaccharides recovered in the hydrolysate were determined using high-pressure size exclusion chromatography coupled to refraction index detector (HPSEC-RID). Briefly, the 1260 HPLC system (Agilent Technologies, CA, USA) consisted of a PL Aquagel-OH guard precolumn (Agilent Technologies, CA, USA) linked in series with PL Aquagel-OH 30 and PL Aquagel-OH 40 columns (300 mm × 7.5 mm, particle size 8 μm, Agilent Technologies, CA, USA), coupled to a refractive index detector (RID). Characterization of OSH and samples obtained from the diafiltration process was done at 35 °C. 20 μL of each sample, previously filtered through 0.22 μL syringe filters (Scharlab, Spain), was eluted in isocratic mode using 0.01 M ammonium acetate at a flow rate of 0.7 mL/min as the mobile phase. A set of pullulan standards in the range 0.342–400 kDa (PSS Polymer Standards Service GmbH, Mainz, Germany) were used for calibration. Standards were also filtered through 0.22 μm syringe filters. Data were analysed with Agilent OpenLab Data Analysis 2.5 software.

Determination of phenolic compounds. Each sample was characterized by High Performance Liquid Chromatography using a Diode Array Detector (HPLC-DAD, Agilent 1100, CA, USA) with a Kinetex® Biphenyl column (250 × 4.6 mm, particle size 5 μm, pore size 100 Å) supplied by Phenomenex (CA, USA). The mobile phase consisted of (A) ammonium acetate 5 mM with acetic acid (1 %, v/v) in water and (B) ammonium acetate 5 mM with acetic acid (1 %, v/v) in acetonitrile. The gradient profile was the following: From 0 to 7 min, 2 % of solvent B (isocratic); from 7 to 20 min, from 2 % to 8 % of solvent B; from 20 to 35 min, from 8 % to 10 % of solvent B and from 35 to 55 min, 10 %–18 % of solvent B; from 55 to 65 min, increase from 18 % to 38 % of solvent B; from 65 to 75 min increase up to 65 % of solvent B; from 75 to 80 min increase to 80 % of solvent B. Post time was 10 min. The flow rate was set at 0.8 mL/min and temperature column was 25 °C. Samples were filtered (0.45 μm pore size, Scharlab, Spain) before injection. OpenLab CDS software was employed to collect and analyse the chromatographic data delivered by the diode array detector and the identification of the different phenolic compounds was done by comparing retention times and UV spectrum with those of standards supplied by Sigma-Aldrich (USA). The total phenolic compounds (TPC) were calculated as the sum of the individual phenolics detected at 280 nm.

Zeta potential, density and pH measurements. The zeta potential (ξ) of the samples was measured with a Zetasizer Nano ZS apparatus (Malvern Panalytical, Malvern, United Kingdom), using the Laser Doppler Velocimetry technique and a DTS1061 disposable folded capillary cell. The zeta potential was calculated using Henry's equation and the Smoluchowski approximation [36]. The density of the samples was measured by means of the density-meter DMA 5000 (Anton Paar, Austria). The pH of the samples was measured by means of a pH-meter (Crison GLP 22, Crison Instruments S.A, Spain).

2.6. Data processing

2.6.1. Analysis of membrane fouling

The filtration resistances have been estimated by the resistance-in-series model and Darcy's law (Eq. (3)) using the experimental value of the membrane permeability coefficient ($L_p = J/TMP$):

$$r_T = \frac{1}{L_p \bullet \mu} = r_m + r_f \tag{3}$$

where, r_T is the total resistance to filtration (m^{-1}), r_m is the membrane hydraulic resistance (m^{-1}), r_f is the fouling resistance due to concentration polarisation and fouling effects (m^{-1}), and μ is the permeate viscosity (Pa s).

The filtration of pure water at TMP from 0.25 to 1.5 bar has allowed to know the pure water permeate flux (J_0) as well as the resistance r_m. The contribution of the fouling to the total resistance, r_f/r_T, has also been calculated.

The membrane fouling mechanisms have been examined using the Hermia's model [37] modified by Field [38] for crossflow filtration:

$$\frac{dJ}{dt} = -k \bullet (J - J^*) \bullet J^{2-n} \tag{4}$$

where k, n and J* are the fouling index, the fouling mechanism, and the critical flux that should not be exceeded in order to avoid fouling, respectively. By integrating Eq. (4) with n fixed (0, 1.5 and 2), the following fouling models have been obtained [30]:

$$\ln\left(\frac{J}{J - J^*}\right) - \frac{J^*}{J} = \left[\frac{J^*}{J_0} - \ln\left(\frac{J_0 - J^*}{J_0}\right)\right] + k_{cl} \bullet J^{*2} \bullet t \ (\text{for } n = 0, \text{cake layer formation}) \tag{5}$$

$$\frac{1}{J^{0.5}} = \frac{1}{J_0^{0.5}} + k_s \bullet t \ (\text{for } n = 1.5, \text{standard blocking}) \tag{6}$$

$$\ln(J - J^*) = \ln(J_0 - J^*) - k_c \bullet t \ (\text{for } n = 2, \text{complete blocking}) \tag{7}$$

where k_{cl} k_s, and k_c are the fouling indexes for cake layer formation (m^{-2} s), standard pore-blocking ($m^{-0.5}$ $s^{-0.5}$), and complete blocking (s^{-1}) models, respectively. Equations (5)–(7) have been employed to model the experimental permeate flux profile, and the predominant fouling mechanisms during OSH filtration have been identified by comparing

the determination coefficient, R^2 [27,30,39].

2.6.2. Process parameters

The yield and purity results of filtration experiments have been calculated as the percentage variation of retentate and permeate content relative to the initial OSH content. The retention coefficients of different OSH compound, R_i, were determined as follows:

$$R_i\ (\%) = \left(1 - \frac{C_{i(p)}}{C_{i(F)}}\right) \bullet 100 \tag{8}$$

and transmission coefficients, T_i, as:

$$T_i(\%) = \frac{C_{i(p)}}{C_{i(r)}} \bullet 100 \tag{9}$$

where C_i (g/L) is the compound concentration, and subscripts p, r and F refer to the permeate, retentate and feed solution, respectively.

The selectivity, α, of ultrafiltration between POS fraction and other OSH compounds (j) was estimated as:

$$\alpha = \frac{T_j}{T_{POS}} \tag{10}$$

2.6.3. Mathematical formulation for diafiltration data analysis

The concentration in the permeate of the OSH compounds ($C_{i(p)}$) during diafiltration has been estimated using the governing mass balance in the feed tank (Eq. (11)).

$$V_r \bullet \frac{dC_{i(r)}}{dt} = -A \bullet J \bullet C_{i(p)} \tag{11}$$

By combining Eq. (11) and Hermia's model (Eq. (4)), $C_{i(p)}$ in the course of the diafiltration can be expressed as follows:

$$\frac{dC_{i(p)}}{dJ} = \frac{A \bullet \overline{T_i} \bullet J}{V_r \bullet k \bullet (J - J^*) \bullet J^{2-n}} \bullet C_{i(p)} \tag{12}$$

where A is the membrane area, V_r is the retentate volume, $\overline{T_i}$ is the average transmission coefficient of the different OSH compounds during all diafiltration operation (Eq. (9)), J is the permeate flux, and J*, n and k are parameters of the Hermia's model (Eq. (4)). When the fouling mechanism (n = 0, 1.5 or 2) is fixed, the following linearised models (Eqs. (13)–(15)) were obtained by integrating Eq. (12) from J_0 to J and from $C_{i(p)0}$ to $C_{i(p)}$ as the boundary conditions:

$$\ln(C_{i(p)}) = \ln(C_{i(p)0}) + \frac{A \bullet \overline{T_i}}{V_r \bullet J^* \bullet k_{cl}} \bullet \ln\left(\frac{J_0 \bullet (J - J^*)}{J \bullet (J_0 - J^*)}\right) \text{ (for n = 0, cake layer formation)} \tag{13}$$

$$\ln(C_{i(p)}) = \ln(C_{i(p)0}) + \frac{A \bullet \overline{T_i}}{V_r \bullet k_s} \bullet \left(\sqrt{J} - \sqrt{J_0}\right) \text{ (for n = 1.5, standard blocking)} \tag{14}$$

$$\ln(C_{i(p)}) = \ln(C_{i(p)0}) + \frac{A \bullet \overline{T_i}}{V_r \bullet k_c} \bullet \left[J - J_0 + J^* \bullet \ln\left(\frac{J - J^*}{J_0 - J^*}\right)\right] \text{ (for n = 2, complete blocking)} \tag{15}$$

In the case of a constant J during all diafiltration process, the following linearised model (Eq. (16)) was obtained by integrating Eq. (11) from t_0 to t and from $C_{i(p)0}$ to $C_{i(p)}$ as the boundary conditions [23]:

$$\ln(C_{i(p)}) = \ln(C_{i(p)0})) - \overline{T_i} \bullet DV \tag{16}$$

Eqs. (13)–(16) have been employed to fit the experimental $C_{i(p)}$ kinetic data and to estimate retention coefficients during diafiltration. The determination coefficients were used to assess the goodness of fit of the diafiltration kinetic models.

Table 1
Physico-chemical characterisation of the onion skin hydrolysate (OSH). N.D.: not detected.

	COMPOSITION
Total pectic oligosaccharides (POS, g/L)	5.17 ± 0.06
Galacturonic acid (g/L)	3.94 ± 0.02
Galactose (g/L)	0.486 ± 0.006
Glucose (g/L)	0.30 ± 0.02
Xylose (g/L)	0.069 ± 0.001
Rhamnose (g/L)	0.369 ± 0.008
Arabinose (g/L)	0.005 ± 0.001
Free galacturonic acid (GA, g/L)	0.324 ± 0.004
Free galactose (gal, g/L)	0.09 ± 0.01
Free glucose (glu, g/L)	0.296 ± 0.007
Free xylose (xyl, g/L)	0.188 ± 0.005
Free rhamnose (rha, g/L)	N.D.
Free arabinose (ara, g/L)	0.124 ± 0.007
Formic acid (FA, g/L)	0.47 ± 0.01
Acetic acid (AcA, g/L)	0.12 ± 0.01
Total phenolic compounds (TPC, g/L)	0.280 ± 0.002
Furfural (F, mg/L)	0.041 ± 0.002
Hydroxymethylfurfural (HMF, g/L)	0.008 ± 0.001
Total solids (g/L)	7.5 ± 0.6
Density at 25 °C (g/L)	1002 ± 2
Zeta potential (ξ, mV)	−12.3 ± 0.5
pH	3.76 ± 0.06

2.6.4. Statistical analysis

All the statistical processing of the experimental data was done using Statgraphics Centurion 19-X64 package (Statistical graph Co., Rockville, MD, USA). Each experiment was carried out at least three times. The permeates and retentates collected throughout diafiltration, the feed solution, the final permeate, and the final retentate were analysed in triplicate. Concentrations in the retentate were also calculated by mass balances, with errors less than 1.5 % for all analysed compounds. The standard deviation (SD) was used to assess the degree of dispersion for the experiments under the same operating conditions and to validate the data. The significance of the differences was determined based on an analysis of variance with the Fisher's least significant difference (LSD) procedure at a p-value ≤0.05.

3. Results and discussions

3.1. Onion skin hydrolysate composition

The results of the physicochemical characterisation of the onion skin hydrolysate (OSH) are presented in Table 1. OSH has been characterized as a complex acidic aqueous solution with a pH of 3.76 ± 0.06 and a negative zeta potential of −12.3 ± 0.5 mV. The total pectic oligosaccharides (POS) derived from the subcritical water hydrolysis of onion skin pectin were found to be 5.17 ± 0.06 g/L, with galacturonic acid

being the predominant component among the oligomers (76.2 %), followed by neutral sugars in variable composition, ranging from 0.069 ± 0.001 g/L of xylose (1.3 %), 0.005 ± 0.001 g/L of arabinose (0.1 %), 0.30 ± 0.02 g/L of glucose (5.9 %), to 0.369 ± 0.008 mg/L of rhamnose (7.1 %), and up to 0.486 ± 0.006 g/L of galactose (9.4 %). Total rhamnose content in the hydrolysate comes from the oligomers, as no free rhamnose was detected. Furthermore, glucuronic acid oligomers and free glucuronic acid were absent in the hydrolysate.

In addition to the pectic oligosaccharide (POS) fraction, it was detected the presence of 0.324 ± 0.004 g/L of free galacturonic acid (7.6 % of the total galacturonic acid in the hydrolysate) and 0.59 ± 0.01 g/L of organic acids, consisting of 79.6 % formic acid and 20.3 % acetic acid. It has also been identified 0.70 ± 0.01 g/L of free monosaccharides, including 12.9 % galactose, 26.9 % xylose, 17.8 % arabinose, and 42.4 % glucose, as well as a minor quantity of hydroxymethyl furfural (0.008 ± 0.001 g/L) and furfural (0.041 ± 0.002 g/L). These findings align with the degradation products previously reported by Gómez et al. [15] in the context of SubW biomass hydrolysis. They observed minimal amounts of hydroxymethyl furfural and furfural when the SubW hydrolysis of lemon peels was carried out below 160 °C. However, when the SubW temperature was raised to 180 °C, the concentration of free galacturonic acid, galactose, arabinose, xylose, and rhamnose in the reaction liquor increased, as a consequence of the hydrolytic reaction, which also led to higher concentrations of organic acids and furfural. Pińkowska et al. [40] also detected a low furfural content in the SubW hydrolysates from a high methyl ester citrus-apple pectin using an operating temperature between 120 and 150 °C, observing an increase in the content of degradation products with the increase in temperature. Martínez et al. [41] reported comparable results, identifying free monosaccharides, formic acid, and acetic acid as the major impurities in the POS production from orange peel waste using a SubW treatment below 160 °C. The total content of phenolic compounds was quantified at 0.280 ± 0.002 g/L. For a detailed profile of phenolic compounds, refer to Table S1 in the supplementary material section. The primary phenolic compounds present in the hydrolysate were p-hydroxybenzoic acid (57.5 wt%), protocatechuic acid (25.7 wt%), and quercetin 4′-glucoside (11.2 wt%).

The molecular weight (MW) distribution of the POS fraction recovered in the hydrolysate was also examined and it is presented in Fig. 3A. As can be observed, various galacturonic acid species were identified based on their molecular weights, ranging from about 150 to 0.2 kDa. The most prevalent pectin-derived oligosaccharides (peaks 1 and 2, 55.5 % of the total area) exhibited an average molecular size exceeding 20 kDa, followed by an intermediate fraction (peaks 3 and 4), constituting approximately 32.2 % of the total area, with a molecular size in the range between 20 and 1.5 kDa. Lastly, there was a low molecular weight fraction (peak 5, representing about 12.3 % of the total area) with a molecular size below 0.5 kDa, corresponding to free galacturonic acid and other structures (galacturonic acid dimers and trimers). These findings highlight the potential of investigating crossflow ultrafiltration in diafiltration mode using various membrane cutoff values between 1 and 100 kDa to explore the fractionation and purification of POS species in terms of molecular weight.

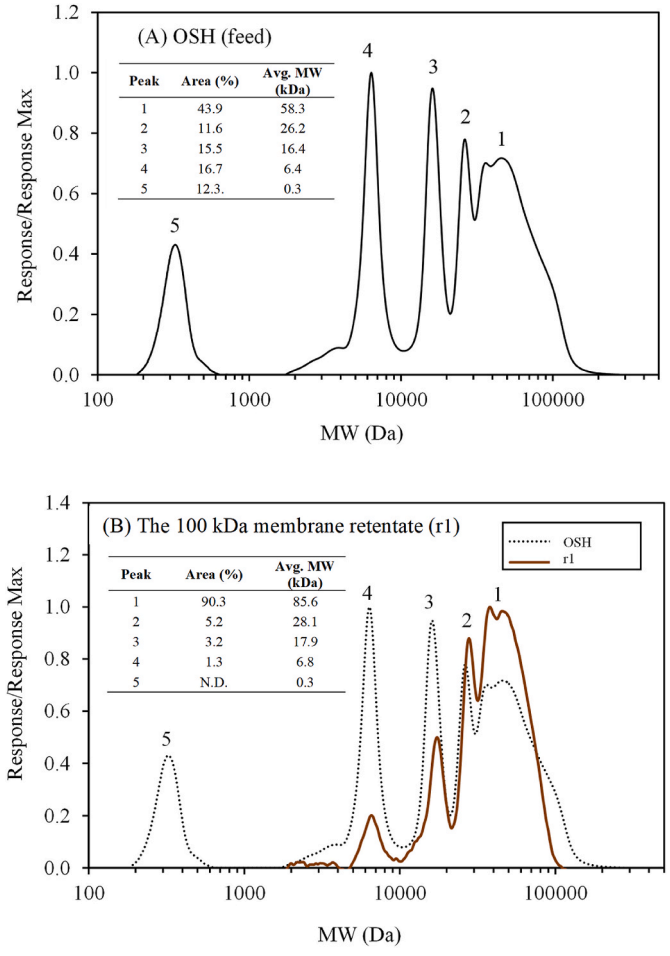

Fig. 3. Molecular weight (MW) distribution of the galacturonic acid species in (A) the onion skin hydrolysate (OSH) used as feed solution in this work, and (B) in the retentate (r1) obtained by OSH diafiltration through a 100 kDa membrane at 25 °C, TMP = 1 bar, CFV = 1.5 m $s^{-1}$and 6.2 diafiltration volumes.

3.2. Ultrafiltration of OSH in total recirculation mode

The effect of the membrane molecular weight cutoff size on the separation of different compounds of the OSH, and fouling has been examined. A comprehensive examination of the principal mechanisms causing membrane fouling is also essential in order to enhance the performance of OSH ultrafiltration. For this purpose, the hydrolysate and deionised water (conductivity ≤15 μS/cm) underwent ultrafiltration in total recirculation mode with different cutoff-sized membranes from 1 kDa to 100 kDa. Prior to this experimental study, a start-up of the ultrafiltration process was carried out with the evaluation of the influence of the transmembrane pressure on the permeate flux.

3.2.1. Effect of the transmembrane pressure on the membrane performance

To initiate the ultrafiltration process, the transmembrane pressure (TMP) was gradually raised from 0.25 to 1.5 bar during the filtration of both pure water and the OSH in total recirculation mode using 1, 10, 50, and 100 kDa cutoff-sized membranes at 25 °C and CFV = 1.5 m s^{-1}. The effect of TMP on the permeate flux during the start-up experiments is depicted in Fig. S1. The permeate flux of pure water (J_0) exhibited a linear increase with rising TMP within the 0.25–1.5 bar range. The permeability coefficients for pure water, denoted as Lp_0, were as follows: 15.1, 96.6, 119 and 132 L bar^{-1} h^{-1} m^{-2} for the 1, 10, 50, and 100 kDa membranes, respectively. As a general trend, membrane permeability was considerably lower for the OSH compared to pure water, with the differences being more pronounced at the highest applied pressures for all membranes. When filtering the onion skin OSH, it was observed that the permeate flux (J) and TMP did not maintain a linear relationship. J initially increased linearly with TMP, then began to stabilise at 0.8–1 bar, and remained constant between 1 and 1.5 bar for all membranes. The non-linear behaviour of J with the driven force is usually associated with the formation of saccharide cake layers on the membrane surface and the compression of deposited cakes [26,42,43]. Moritz et al. [34] found that fouling layers are formed rapidly when the feed solution and membrane surface presented opposite charge, as in the OSH filtration (ξ = − 12.3 mV) where the membrane surface was positively charged at the experimental pH. Bacchin et al. [44] have reported that the limiting flux corresponds to the permeate flux at which the membrane filtration

capacity is saturated due to fouling. Additionally, fouling caused by the hydrolysate became more severe when the limiting flux was reached, resulting the fouling resistance (r_f, Eq. (3)) and its contribution to the total resistance (r_f/r_T, %) increasing at a rate proportional to the driving force for all the membranes, as shown in Fig. S2. These resistance results confirm that permeation through the 1–100 kDa membranes was in the diffusion-controlled region at high TMP. In this regard, the limiting flux was reached at a TMP of only 1 bar, suggesting that higher values should not be recommended for onion skin hydrolysate filtration in order to reduce the membrane cleaning frequency in continuous UF processes as well as to prevent energy waste.

3.2.2. *Effect of the membrane molecular weight cutoff on the OSH fractionation and fouling*

Following the determination of the operational TMP at 1 bar, the subsequent stage involved investigating the influence of the membrane molecular weight cutoff (MWCO) on the separation efficiency of pectic oligosaccharides (POS) from other compounds present in the OSH and fouling characterisation. The results of the hydrolysate underwent ultrafiltration in total recirculation mode at 25 °C, TMP = 1 bar, and CFV = 1.5 m s^{-1} with different cutoff-sized membranes from 1 kDa to 100 kDa are presented in Fig. 4 and in Table 2: encompassing the experimental data corresponding to the membrane retention and selectivity at the end of filtration (Fig. 4A and B), permeate flux over time (Fig. 4C), and parameters for fouling characterisation (Fig. 4D and Table 2).

Fig. 4A illustrates that the ceramic membranes from 1 to 100 kDa achieved acceptably high retention (R_i, Eq. (8)) of the total POS fraction present in the OSH. A noticeable correlation between membrane MWCO and POS retention was observed, although slight differences were found between 50 kDa and 100 kDa cutoff sizes. POS retention was approximately 50 % using the membranes with the highest cutoff sizes. When the membrane cutoff size was reduced to 10 kDa, POS retention increased to approximately 70 %, and further rose to above 80 % with the use of a 1 kDa membrane. The comparison of retention results with the POS molecular size distribution presented in Fig. 3 reveals that it has been possible to obtain a complete retention of the largest POS (peaks 1 and 2) with all membranes, a good retention of the intermediate POS ranging from about 20 to 10 kDa (peak 3) using the membranes with the lowest cutoff sizes, while the POS fraction with a molecular size between 10 and 1.5 kDa (peak 4) was exclusively retained by the 1 kDa membrane. According to a previous work [14], pectin oligomers from onion skin solid residues preserved the branched domains of ramnogalacturonan type I (RG-I) when using an extraction process with SubW at 145 °C. This result was also observed in this work (Table 1), where rhamnose and neutral sugars have been identified in oligomeric form and free rhamnose was not detected in the hydrolysate. It should also be

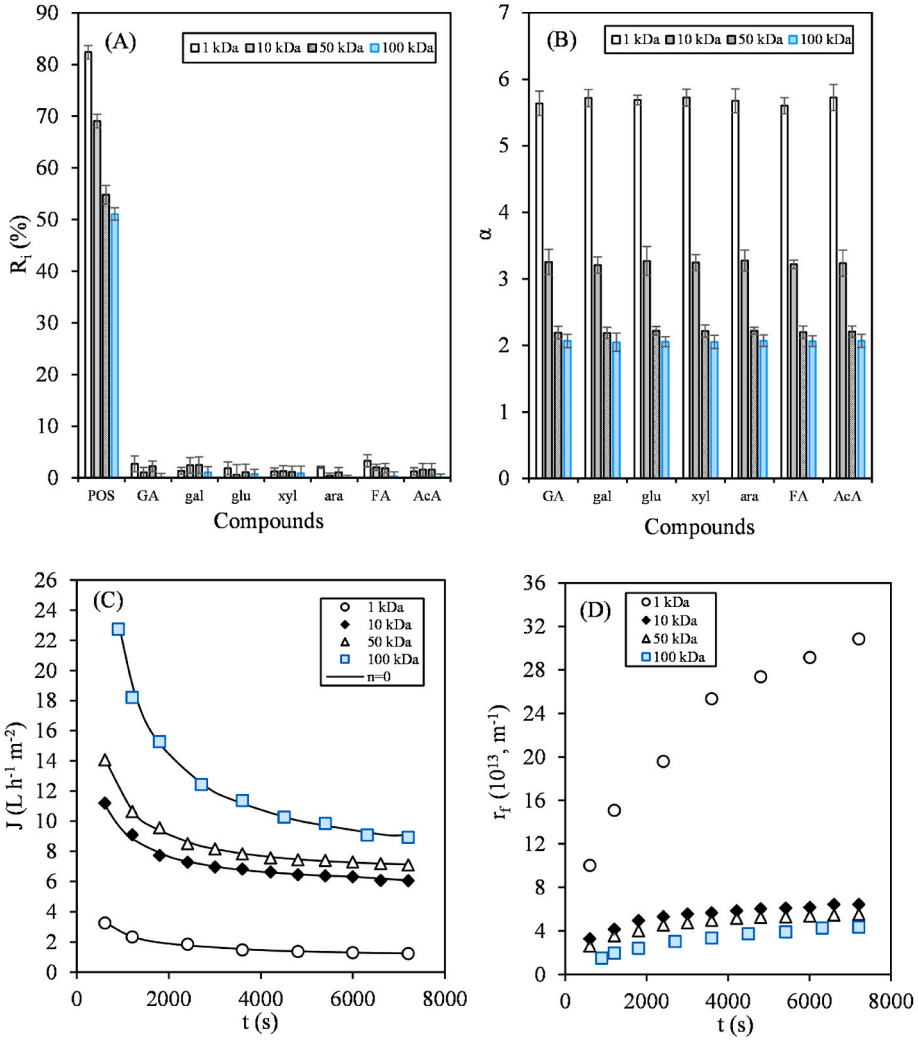

Fig. 4. Effect of the membrane molecular weight cutoff size (1–100 kDa) on the OSH filtration in total recirculation mode at 25 °C, TMP = 1 bar and CFV = 1.5 m s^{-1}. (A) Retention coefficients (R_i, Eq. (8)) for pectic oligosaccharides (POS), free galacturonic acid (GA), galactose (gal), glucose (glu), xylose (xyl), arabinose (ara), formic acid (FA) and acetic acid (AcA) at the end of filtration. (B) Membrane selectivity (α, Eq. (10)) towards total POS fraction. (C) Permeate flux (J) profile modelled by Hermia's cake layer model (Eq. (5), n = 0). (D) Evolution of fouling resistance (r_f, by Eq. (3)) along filtration.

Table 2
Experimental parameters, filtration resistances (r_T, r_m, and r_f, Eq. 3) and foiling indexes (k_c, k_s and k_{cl}) of three Hermia's fouling models (Eqs. 5, 6 and 7) for the OSH ultrafiltration in total recirculation mode with different cutoff-sized membranes from 1 to 100 kDa at 25 °C, TMP = 1 bar and CFV = 1.5 m s^{-1}.

PARAMETERS	1 kDa	10 kDa	50 kDa	100 kDa
J_0 (L $h^{-1}m^{-2}$)	15.1 ± 0.2	96.6 ± 0.5	96.6 ± 0.5	132.0 ± 0.5
J (L $h^{-1}m^{-2}$)	3.3–1.2 ± 0.1	11.2–6.1 ± 0.2	14.1–7.1 ± 0.3	22.8–8.9 ± 0.2
r_m (10^{12} m^{-1})	2.8	4.3	3.5	3.2
r_f (10^{12} m^{-1})	100.1–308.8	32.9–64.4	26.1–55.3	15.2–43.5
r_f/ r_T (%)	78–92	88–94	88–94	83–93
k_{cl} (n = 0, Eq. (5), s m^{-2})	$153.9{\cdot}10^{7}$	$13.4{\cdot}10^{7}$	$9.6{\cdot}10^{7}$	$3.0{\cdot}10^{7}$
R^2 (n = 0, Eq. (5))	0.994	0.995	0.993	0.993
k_s (n = 1.5, Eq. (6), $s^{-0.5}m^{-0.5}$)	0.09	0.03	0.03	0.03
R^2 (n = 1.5, Eq. (6))	0.891	0.807	0.781	0.907
k_c (n = 2, Eq. (7), s^{-1})	$3.3{\cdot}10^{-4}$	$5.4{\cdot}10^{-4}$	$5.0{\cdot}10^{-4}$	$3.3{\cdot}10^{-4}$
R^2 (n = 2, Eq. (7))	0.945	0.974	0.973	0.956
T_{POS} (%)	17 ± 1	30.4 ± 0.8	45 ± 1	48 ± 2
T_{GA} (%)	97 ± 2	99 ± 2	98 ± 1	99.8 ± 0.6
T_{gal} (%)	98.6 ± 0.9	98 ± 1	97.5 ± 0.8	98.9 ± 0.8
T_{glu} (%)	98.1 ± 0.4	99 ± 1	99 ± 2	99.2 ± 0.7
T_{xyl} (%)	98.7 ± 0.7	99 ± 1	98.8 ± 0.7	99.1 ± 0.7
T_{ara} (%)	98 ± 1	99.6 ± 0.5	98.9 ± 0.5	100 ± 1
T_{FA} (%)	97 ± 2	97.9 ± 0.8	98 ± 1	99.7 ± 0.8
T_{AcA} (%)	98.7 ± 0.5	98 ± 1	98 ± 2	99.9 ± 0.5
$pH_{(r)}$	3.78 ± 0.07	3.8 ± 0.1	3.8 ± 0.1	3.7 ± 0.1
$\xi_{(r)}$ (mV)	−12.1 ± 0.6	−12.8 ± 0.5	−12.8 ± 0.6	−12.4 ± 0.6

J_0: pure water permeate flux; J: permeate flux; R^2: determination coefficient of Hermia's models; T: transmission coefficients at the end of filtration estimated by Eq. (9); $pH_{(r)}$: retentate pH and $\xi_{(r)}$: retentate zeta potential; POS: pectic oligosaccharides; GA: free galacturonic acid; gal: galactose; glu: glucose; xyl: xylose; ara: arabinose; FA: formic acid; AcA: acetic acid.

considered that the largest POS with less hydrolysed RG-I branches exhibit a more complex "hairy" spatial configuration [45–47] and steric interactions may hinder their passage through the membrane pore [48], which was probably a significant contribution to their decreased transport throughout the 50 and 100 kDa membranes.

Regarding the separation efficiency, as depicted in Fig. 4A, the highest retention values corresponded to the POS species. In addition, retention values below 3 % were obtained for monosaccharides, free galacturonic acid and organic acids with all membranes, indicating that the pore size distribution of the 1 kDa membrane also proved to be large enough to allow complete transport of low-molecular-weight compounds (impurities) present in the OSH. This result was validated by the membrane selectivity (α, Eq. (10)) in Fig. 4B, observing that these UF membranes were selective for the POS separation from the different free monosaccharides and organic acids with values above 5 for the lowest membrane cutoff and approximately 2 for the highest membrane cutoff. The reduction in selectivity was only due to the POS increased transport (T_i, Eq. 9) from 17 % to 48 % when increasing the molecular weight cutoff size of the membrane from 1 to 100 kDa, as can be observed in Table 2. Consequently, these results suggest that it is feasible to achieve a selective separation of POS species, as these low-molecular-weight compounds can pass through the membrane regardless the UF membrane cutoff size used.

In the case of the permeate flux (J), Fig. 4C shows that J was sharply reduced by decreasing the molecular weight cutoff size of the membrane from 100 to 1 kDa. A fast J loss took place at the beginning of the UF with all membranes due to the build-up of the polarisation boundary layer, followed by a slow J decrease during 30–90 min, and then J remained mostly constant at around 8.9 L h^{-1} m^{-2} for the membranes with the highest cutoff sizes and close to 1.2 L h^{-1} m^{-2} for the membranes with the lowest cutoff sizes. It can be observed from Table 2 that the fouling resistance (r_f) was considerably higher than the membrane resistance (r_m) in all experiments, suggesting that concentration polarisation and fouling were the predominant contributions to the flux decline. Due to the negligible retention of the most abundant OSH impurities (Fig. 4A), it can be assumed that the POS fraction was, hence, the primary foulant responsible for the r_f increase and J drop during OSH filtration. To comprehend the fouling mechanisms affecting filtration performance, Hermia's models (Eqs. (5)–(7)) were used. The experimental J data were analysed by fitting with each model and the results of fouling indexes (k_c, k_s and k_{cl}) along with the R^2 coefficients are listed in Table 2. Considering the results presented in Tables 2 and in Fig. 4C, the cake layer formation model (Eq. (5) for n = 0, R^2 = 0.993, 0.993, 0.995 and 0.994 for the 100, 50, 10 and 1 kDa membranes, respectively) provided the best fit to the experimental J data. This result justifies that the fouling occurred predominantly on the membrane surface, resulting the J decrease and the r_f increase (Fig. 4D) controlled by the POS cake layer formation, with low contribution of the pore blockage. It should be noted that cake layer formation has already been identified as the main contribution to irreversible fouling in the filtration of different pectin solutions. Gimenes et al. [49] used Hermia's models and identified cake layer formation as the dominant restrictive fouling mechanism during the filtration of aqueous pectin solutions, achieving retention coefficients of up to 97.8 %. Similarly, Xie et al. [50] observed gel layer formation on the membrane surface as the primary cause of permeate flux decline in the filtration of pectin solutions derived from citrus peels. In contrast, Echavarria et al. [29] found that apple pectin, ranging from 50 to 1200 kDa, formed thick gel layers that led to pore clogging during the filtration through a 100 kDa membrane. Rai et al. [51] proposed a surface interaction between pectin and the pores, resulting in pore sealing due to the deposition of pectin on the membrane surface in the form of gel. Sarkar [52] also identified simultaneous cake layer formation and complete pore blocking during the filtration of pectin solutions ranging from 30 to 100 kDa using a 30 kDa membrane. However, the low contribution of complete pore blocking resistance ($R^2 \leq 0.97$ for all membranes, Table 2) observed in this work suggests a low degree of pore sealing due to the low adhesion of the POS gel layer to the membrane surface. In addition, the comparison of k_{cl} indexes revealed that the reduction of the membrane MWCO from 100 to 1 kDa leads to a high increase in cake layer resistance due to the increased concentration polarisation and the decreased back-diffusion, which resulted in increased POS deposition on the membrane surface and the formation of thicker and less porous cake layers during filtration. Therefore, these results suggest that to minimise the severe surface fouling caused by pectin-derived oligosaccharides, it may be more desirable to start the OSH fractionation process with the

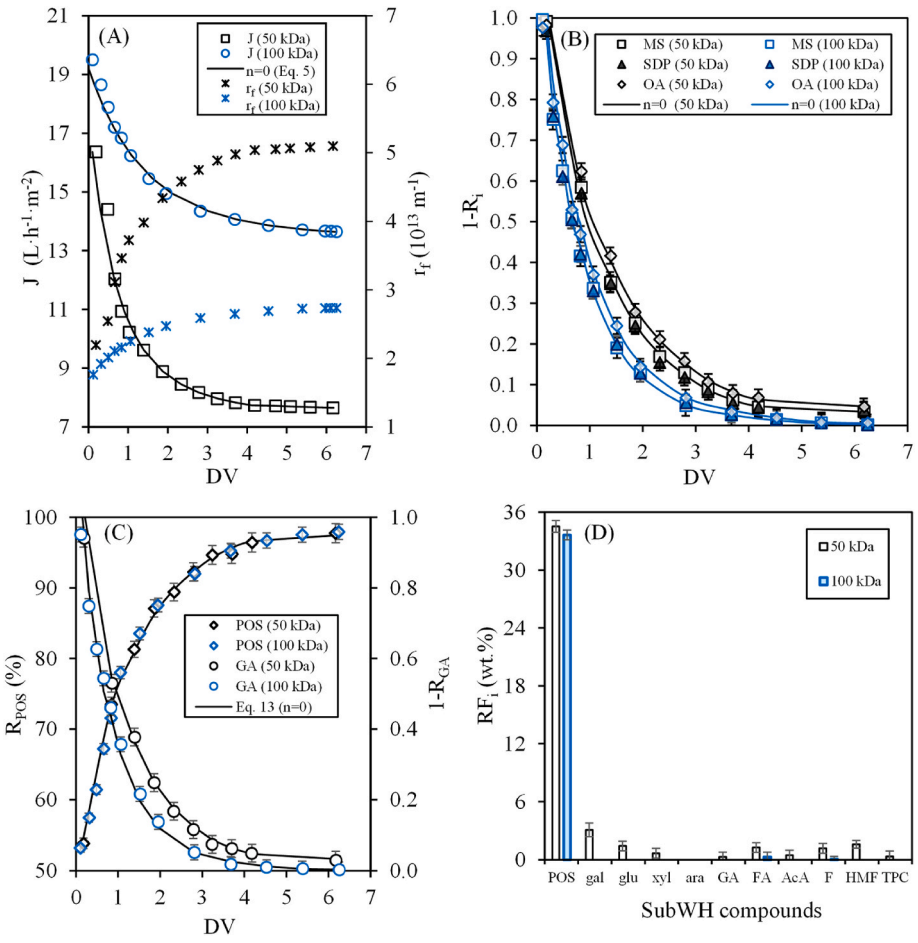

Fig. 5. Results of the OSH diafiltration using the 50 and 100 kDa membranes at 25 °C, TMP = 1 bar, CFV = 1.5 m s^{-1}. (A) Permeate flux (J) and fouling resistance (r_f, Eq. (3)) versus diafiltration volume (DV) along diafiltration and J profiles modelled by Hermia's cake layer model (Eq. (5), n = 0). (B) The removal (1-R_i, Eq. (8)) of monosaccharides (MS), organic acids (OA) and sugar dehydration products (SDP) versus DV along diafiltration and their profiles modelled by Eq. 13. (C) The retention of pectic oligosaccharides (POS) and the removal of free galacturonic acid (GA) versus DV along diafiltration and their profiles modelled by Eq. 13. (D) Recovery factors (RF_i) at the end of diafiltration calculated as the percentage variation of the retentate content relative to the initial OSH content.

Table 3
Determination coefficients (R^2) and foiling indexes (k_c, k_s and k_{cl}) for the OSH diafiltration using the 50 and 100 kDa cutoff-sized membranes at 25 °C, TMP = 1 bar and CFV = 1.5 m s^{-1}, calculated from the permeate flux profile (J) of Fig. 5A (Eqs. (5)–(7)) and from the removal profiles (1-R_i) of Fig. 5B and C (Eqs. (13)–(15)).

MEMBRANE (kDa)	COMPOUNDS AND DATA PROFILE		$\overline{T}_i$ (±1 %)	CAKE LAYER FORMATION (n = 0)		STANDARD PORE BLOCKING (n = 1.5)		COMPLETE PORE BLOCKING (n = 2)	
				k_{cl} (s m^{-2})	R^2	k_s ($s^{-0.5}m^{-0.5}$)	R^2	k_c (s^{-1})	R^2
50		J		$3.43{\cdot}10^{7}$	0.999	–	0.801	$2.1{\cdot}10^{-4}$	0.975
50	MS	1-R_i	64	$3.44{\cdot}10^{7}$	0.998	–	0.712	$2.4{\cdot}10^{-4}$	0.951
50	SDP	1-R_i	64	$3.44{\cdot}10^{7}$	0.995	–	0.613	$2.3{\cdot}10^{-4}$	0.955
50	OA	1-R_i	58	$3.45{\cdot}10^{7}$	0.998	–	0.760	$2.4{\cdot}10^{-4}$	0.948
50	GA	1-R_i	64	$3.42{\cdot}10^{7}$	0.997	–	–	$2.3{\cdot}10^{-4}$	0.945
100		J		$0.84{\cdot}10^{7}$	0.998	–	0.819	$1.4{\cdot}10^{-4}$	0.988
100	MS	1-R_i	86	$0.83{\cdot}10^{7}$	0.993	–	0.799	$1.5{\cdot}10^{-4}$	0.982
100	SDP	1-R_i	86	$0.83{\cdot}10^{7}$	0.991	–	0.787	$1.4{\cdot}10^{-4}$	0.978
100	OA	1-R_i	79	$0.84{\cdot}10^{7}$	0.992	–	0.794	$1.5{\cdot}10^{-4}$	0.980
100	GA	1-R_i	86	$0.84{\cdot}10^{7}$	0.994	–	–	$1.5{\cdot}10^{-4}$	0.986

J: permeate flux; R_i: retention coefficient (Eq. 8); $\overline{T}_i$: average transmission coefficient during diafiltration (Eqs. (13)–(15)); GA: free galacturonic acid; MS: free monosaccharides; OA: organic acids; SDP: sugar dehydration products.

100 kDa membrane, even though the average molecular size of the largest POS in the hydrolysate has turned out to be only 58.3 kDa. Based on these results, 50 and 100 kDa membranes were selected for subsequent diafiltration experiments in order to better compare their separation properties.

3.3. Continuous feed diafiltration of OSH using wide membrane pores (50 and 100 kDa)

Continuous feed diafiltration as a purification process requires maximise yield and purity of the target POS as well as fast removals of

low-molecular-weight impurities in order to minimise the water consumption. The total recirculation experiments have provided evidence that the primary fouling mechanism governing the UF process and permeate flux loss was the POS cake layer formation (n = 0), as indicated by the application of Hermia's model. Consequently, membrane fouling can cause additional resistances to filtration with high impact on diafiltration productivity. Since 50 and 100 kDa membranes have exhibited similar separation properties in total recirculation experiments, the following step has been focused on analysing the hydrolysate fractionation by diafiltration with both membranes. Results of the OSH filtration in diafiltration mode using the 50 and 100 kDa membranes at 25 °C, TMP = 1 bar and CFV = 1.5 m s^{-1} are presented in Fig. 5 and Table 3.

3.3.1. Permeate flux and fouling

The permeate flux (J) and fouling resistance (r_f, Eq.3) are plotted against the diafiltration volume (DV) in Fig. 5A. Permeate flux was considerably lower for the 50 kDa membrane than for the 100 kDa membrane, with low flux differences close to 15 % at the beginning of filtration and slightly above 40 % at the end of filtration (DV = 6.2 L water/L feed). The trend of flux drop with DV was similar with both membranes. It was observed that the most pronounced flux decline took place at low DV from 0.1 to 1 L water/L feed, with a J loss about 37 % for the 50 kDa membrane and slightly above 15 % for the 100 kDa membrane. The flux continued decreasing for DV from 1 to 4.5–5 L water/L feed and then remained constant at around 7.7 L h^{-1} m^{-2} ($r_f = 5.1{\cdot}10^{13}$ m^{-1} and $r_m = 0.35{\cdot}10^{13}$ m^{-1}) for the 50 kDa membrane and about 13.7 L h^{-1} m^{-2} ($r_f = 2.7{\cdot}10^{13}$ m^{-1} and $r_m = 0.32{\cdot}10^{13}$ m^{-1}) for the 100 kDa membrane. The comparison with the r_f results obtained for the OSH filtration in total recirculation mode (Table 2) leads to the conclusion that the fouling build-up was significantly reduced when the OSH was ultrafiltered in diafiltration mode. This means that the dilution effect of the feed concentration (due to the continuous addition of water in the feed tank and solute removal) during diafiltration seems to play a favourable role in limiting fouling phenomena [53]. The experimental flux profiles were analysed by fitting with Hermia's model (Eqs. (5)–(7)) and the results are summarised in Tables 3 and in Fig. 5A. As in the total recirculation experiments, Eq. (5) (n = 0, $R^2 = 0.999$ and 0.998 for the 50 and 100 kDa membranes, respectively) provided the best fit to the experimental J data with the POS cake layer formation as the main fouling contribution to the r_f increase and J loss. The differences in k_{cl} values between the two operation modes and both membranes (Tables 2 and 3) have revealed a high decrease in cake layer resistance for the continuous feed diafiltration and with the 100 kDa membrane, which reinforces the idea of a reduction of POS accumulation over the membrane surface and the formation of thinner and less compacted cake layers when the OSH was diafiltered across the 100 kDa membrane.

3.3.2. Purification degree of pectic oligosaccharides (POS) during ultrafiltration

Free monosaccharides and organic acids (Table 1) have been identified as the major impurities in the OSH used as feed solution in this work. Sugar dehydration products (furfural and HMF) were found in low concentration in this hydrolysate, but their toxicological effects and low acceptable daily intake (<0.5 mg/kg bw) highlight the importance of minimising their concentrations in new formulations of POS products. In this sense, the POS purification study has been carried out by examining the removal of the three groups of compounds: free monosaccharides (MS), organic acids (OA) and sugar dehydration products (SDP).

The removal results ($1\text{-}R_i = C_{i(p)}/C_{i(r)}$, Fig. 5B) obtained for these groups of compounds with both membranes demonstrated that a diafiltration volume (DV) of about 3 L water/L feed provided an oligosaccharide purification above 90 % when using the 100 kDa membrane. This was attributed to the most effective removal of most impurities, with free monosaccharides and sugar dehydration products being removed more rapidly than organic acids. The experimental $1\text{-}R_i$ profiles in Fig. 5B were analysed by fitting with mass balance models (Eqs. (13)–(15)) and the results are summarised in Table 3. The good agreement between the experimental $1\text{-}R_i$ data (symbols) and the data calculated by Eq. (13) (lines) in Fig. 5B justifies that the removal of monosaccharides, organic acids, and sugar dehydration products during the hydrolysate diafiltration depended more on the fouling effects than on the feed dilution effect. The evaluation of the average transmission coefficients ($\overline{T}_i$, Table 3) from the slope of Eq. (13) revealed a significant rejection of these monomeric compounds by the membrane during diafiltration, owing to fouling phenomena. The values of $\overline{T}_i$ were experimentally validated, and no significant differences ($p > 0.05$) were found between the experimental and calculated values according to statistical analysis. Consequently, the transport rate of monomeric compounds across the membrane was slower than expected, and it was especially evident during the diafiltration process with the 50 kDa membrane. In addition, while monosaccharides and dehydration products have shown the highest transport rates ($\overline{T}_{MS} = \overline{T}_{SDP} = \overline{T}_{GA} = 86$ % and 64 % for the 100 and 50 kDa membranes, respectively), organic acids ($\overline{T}_{OA} = 79$ % and 58 % for the 100 and 50 kDa membranes, respectively) have diffused more slowly through these membranes. It should be also considered that the functional carboxylic group of POS was negatively charged at the experimental pH and a considerable fraction of organic acids (mainly formic acid) was also negatively charged and, hence, electrostatic interactions in fouling layers were probably a significant contribution to the slowest transport rate of organic acids during diafiltration process. This effect was also observed by Oueslati et al. [23] for the purification of hyaluronic acid from fermentation broths by continuous feed diafiltration. They achieved a purity level close to 90 % after using a feed-to-water ratio of 7 L/L, attributed to electrostatic interactions with the charged hyaluronic acid in the polarisation layer causing a low diffusion rate of charged impurities through a 100 kDa polyethersulfone membrane.

Consequently, all these results demonstrate that the fouling effects were relatively minimised during the OSH diafiltration with the 100 kDa membrane, achieving a POS purification of more than 90 % with a low diafiltration volume close to 3 L of water per L of feed. Additionally, diafiltration mass balance models have allowed an accurate prediction of POS purification yield during diafiltration. This model also facilitates the identification of average transmission rates across the membrane during the purification process, as well as the predominant fouling mechanisms involved in the treatment of complex mixtures such as OSH.

3.3.3. Fractionation of galacturonic acid species: yield and purity

The experimental data corresponding to the fractionation of the different galacturonic acid species as a function of diafiltration volume (DV) are depicted in Fig. 5C. The 100 kDa membrane provided faster removal of galacturonic acid monomers than the 50 kDa membrane, with no free galacturonic acid detected in either the permeate or the retentate after using a DV close to 5.5 L water/L feed. In the case of POS, no differences in retention coefficients were observed when the membrane cutoff size was increased from 50 to 100 kDa, with a POS retention of approximately 53 % at the beginning of filtration and 98 % at the end of filtration. This implies that a final DV of 6.2 L water/L feed was insufficient to achieve total separation between the largest POS and other POS species with both membranes. As can be observed in Fig. 5C, good agreement was obtained for the retention of POS estimated by Eq. (13) ($R^2 = 0.992$), showing that the transport of the low and intermediate molecular weight POS species throughout the membrane was also controlled by the fouling. It can be concluded that the fractionation level of POS species in terms of molecular weight will dictate the ultimate water consumption of the process. However, a minimum DV can be suggested for the optimisation of the oligosaccharide fractionation process since differences in POS retention were lower than 5 % after using a DV of 3 L water/L feed. This minimal feed-to-water ratio of 3 L/L

aligns with the findings by Cho et al. [54], who selected a diafiltration volume of 2 L water/L feed for pectin separation as a balance between the removal of pectic oligosaccharides and energy consumption for the microfiltration of mandarin peel extracts.

After collecting up to 6.2 diafiltration volumes, the process was stopped, and a successful removal of the three groups of impurities was achieved (>99 %, Fig. 5D) for the filtration with the 100 kDa membrane, as well as the complete removal of the phenolic compounds, that were directly to the permeate stream. Therefore, it can be assumed that the 100 kDa ceramic membrane was also efficient for the POS separation from the phenolic compounds. It has already been reported negligible retentions of ultrafiltration membranes for different profiles of phenolic compounds [55–57]. Alonso-Vázquez et al. [55] found that 95 % of the phenolic compounds from canned mandarin production wastewater were collected in the permeate stream of the ultrafiltration membranes, while its purification and concentration was achieved by nanofiltration. Similar results were observed by Giacobbo et al. [57] for the separation of polysaccharides and phenolic compounds from second racking wine lees. They indicated that ultrafiltration was effective to fractionate polysaccharides and polyphenols, with the polysaccharides mainly stayed in the retentate stream, while phenolic compounds preferentially permeated these membranes. In this context, it is noteworthy that the removal rate of phenolic compounds achieved in this study was considerably faster than that reported by Cho et al. [54]. In their study, even after subjecting the pectin samples to 6 diafiltration volumes with microfiltration membranes, complete removal of these compounds was not achieved.

Furthermore, the final retentate from the 100 kDa membrane after using 6.2 diafiltration volumes (Fig. 5D) accounted for about 34 % of the total POS species present in the OSH. The results of the GPC analysis in Fig. 3B confirmed that the 100 kDa membrane retentate turned out to be a POS product enriched in the largest POS above 30 kDa (peak 1∼90.3 % of the total area), with a slight presence of the POS species ranging from 30 to 1.5 kDa (peaks 2, 3 and 4) and the absence of the smallest galacturonic acid species (peak 5, not detected). Notably, the POS fraction recovered in this retentate was composed of 69.0 mol% of galacturonic acid, 11.3 mol% of rhamnose, and 22.7 mol% of neutral sugars, which indicated a higher degree of branching compared to the total POS in the OSH (Table 4). This was evidenced by an increase in the Rha/GalA ratio (0.14 % compared to 0.1 % in the OSH) and a greater presence of the RG-I domain (36.1 % compared to 28.5 % in the feed, Eq. (2)).

In summary, the 50 kDa and 100 kDa membranes showed similar POS fractionation capacity during the diafiltration process. However, the purification of pectic oligosaccharides, achieved through impurity removal, was clearly less efficient when the MWCO of the membrane was reduced. When using a membrane with a lower MWCO size, increased water addition was necessary to achieve comparable purification levels. Therefore, the 100 kDa membrane was selected as the initial step in a cascade process designed to fractionate pectin-derived oligosaccharides with specific molecular weights.

3.4. Sequential diafiltration for the fractionation of onion skin pectic oligosaccharides

To fractionate the different POS species from the onion skin hydrolysate (OSH), an ultrafiltration-based diafiltration process with sequential UF stages was examined. The sequential diafiltration approach for pectin separation has been previously employed by various researchers [17,20]. Such a strategy has proven effective in achieving substantial removal efficiencies of monosaccharides and other impurities, facilitating the generation of various pectin fractions characterized by different molecular weights.

Based on the results detailed in section 3.3, OSH was diafiltered across the 100 kDa membrane. Subsequently, the permeate from the 100 kDa (p1) underwent further separation, involving the use of 1 kDa and 10 kDa membranes, as illustrated in Fig. 2. The up-scaling of the diafiltration processes must strike a balance between separation degree and water consumption, in order to avoid treating excessive volumes [58]. In this sense, in *Cycle B* was included a concentration stage before the diafiltration stages with 1 and 10 kDa membranes. The entire UF

Table 4
Main features of the final retentates (r1, rA, rB1 and rB2) obtained from the diafiltration cascade processes illustrated in Fig. 2.

		OSH	100 kDa MEMBRANE (Common stage in *Cycles A* and *B*)		*CYCLE A* (1 kDa membrane)	*CYCLE B* (1 and 10 kDa membranes)	
			r1 (100 kDa)	p1 (100 kDa)	rA (1 kDa)	rB1 (10 kDa)	rB2 (1 kDa)
C_{POS} (g/L)		5.17 ± 0.06	1.74 ± 0.01	0.553 ± 0.008	0.471 ± 0.005	0.637 ± 0.004	0.328 ± 0.005
V (±0.01 L)		0.20	0.20	1.24	1.24	0.48	0.76
Purity index (±0.5 wt%)		72.7	99.9	–	92.7	99.8	88.2
RF_{POS} (±0.3 wt%)		–	33.7	66.3	56.5	29.6	24.1
Average MW[a] (Da)		32288	79419	–	20167	35954	7254
MW distribution[a] (kDa)	Peak 1	58.3 (43.9 %)	85.6 (90.3 %)	42.5 (29.7 %)	41.3 (25.5 %)	41.0 (72.2 %)	N.D.
	Peak 2	26.2 (11.6 %)	28.1 (5.2 %)	27.8 (11.8 %)	28.8 (15.1 %)	28.2 (16.2 %)	27.0 (1.4 %)
	Peak 3	16.4 (15.5 %)	17.9 (3.2 %)	16.9 (17.7 %)	17.5 (21.2 %)	17.7 (9.1 %)	16.4 (25.7 %)
	Peak 4	6.4 (16.7 %)	6.8 (1.3 %)	6.6 (23.3 %)	6.6 (23.2 %)	6.9 (2.5 %)	6.5 (39.4 %)
	Peak 5	0.3 (12.3 %)	N.D.	0.3 (17.5 %)	0.3 (15 %)	N.D.	0.3 (33.5 %)
Composition (mol, ±0.1 %)							
GA		74.1	69.0	73.0	74.4	79.5	70.5
glu		5.3	4.8	8.9	5.3	4.7	8.5
xyl		1.5	3.1	0.8	2.0	1.7	1.6
gal		9.0	11.2	7.6	8.9	6.2	9.9
rha		7.9	11.3	6.3	7.3	7.9	6.2
ara		2.3	0.5	3.4	2.1	0.0	3.3
POS Features							
rha/GA (±0.01)		0.10	0.14	0.08	0.10	0.10	0.09
(gal + ara)/rha (±0.01)		1.56	1.12	1.83	1.61	0.87	2.25
HG (±0.1 %)		70.0	60.6	73.1	70.8	75.2	77.4
RG-I (±0.1 %)		28.5	36.1	26.0	27.0	23.0	20.6

OSH: onion skin hydrolysate used as initial feed solution; POS: pectic oligosaccharides; RF_{POS} (wt.%): recovery factor calculated as the percentage variation of the POS content in the retentate or permeate relative to the initial POS content in the OSH. Purity index: POS content relative to the total content of monomeric and oligomeric compounds.

[a] Average molecular weight determined by GPC. In brackets, it is shown the presence of each fraction. N.D.: not detected.

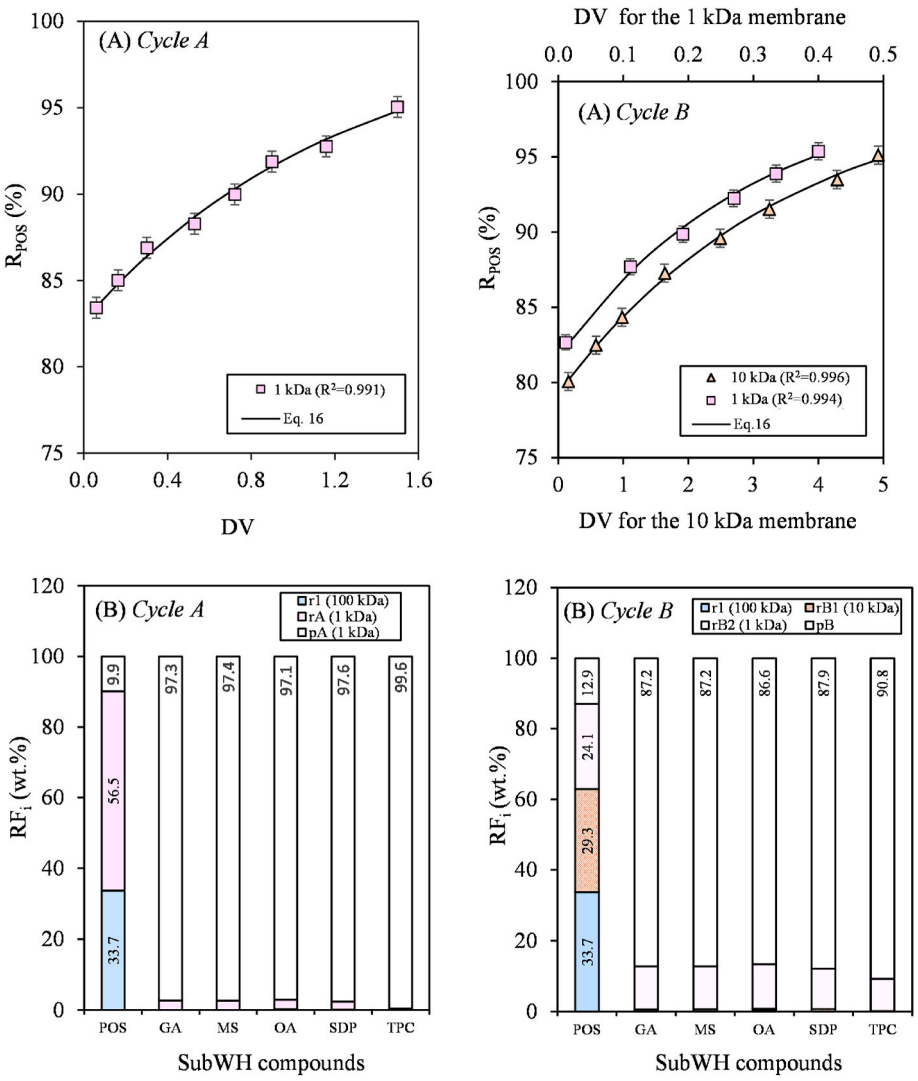

Fig. 6. Results for the diafiltration cascades shown in Fig. 2 (A) The retention of pectic oligosaccharides (POS) versus diafiltration volume (DV) along filtration and their profiles modelled by Eq. 16. (B) Recovery factors (RF_i) at the end of filtration calculated as the percentage variation of retentate content (r1 and rA in *Cycle A;* r1, rB1 and rB2 in *Cycle B*) or permeate content (pA in *Cycle A* and pB in *Cycle* B) relative to the initial OSH content.

processes were conducted at 25 ± 0.1 °C, with a crossflow velocity of 1.5 ± 0.1 m s^{-1} and a transmembrane pressure of 1.0 ± 0.1 bar. It should be indicated that in the first diafiltration stage of *Cycle A* (UF with 100 and 1 kDa membranes) and of *Cycle B* (UF with 100, 10, and 1 kDa membranes), the permeate flux profile for the 100 kDa membrane and the retention of the different OSH components were statistically similar to those shown in Figs. 5 and 3B. A constant permeate flux close to 4.5, 5.3 and 22.1 L h^{-1} m^{-2} was obtained during the diafiltration with the 1 kDa membrane in *Cycle A* and during the diafiltration with the 1 and 10 kDa membranes in *Cycle B*, respectively. The evolution of POS retention with diafiltration volume (DV) for the 1 and 10 kDa diafiltration in these multi-stage cycles is shown in Fig. 6A. Good agreement was obtained for the POS retention estimated by Eq. (16) during the diafiltrations across the 1 and 10 kDa membranes, suggesting that the permeation of low-molecular-weight oligosaccharides through these membranes depended mainly on the dilution feed effect and, to a lesser extent, on the concentration polarisation effects [23,55]. As discussed above, in order to ensure a permeate p1 with the largest fraction of the intermediate POS, the first UF stage (Fig. 5C) was stopped when a DV of 6.2 L of water per litre of OSH was reached. However, in order to minimise water consumption, the final DV for subsequent diafiltrations was experimentally selected as the minimum required to achieve a POS retention close to 95 %, as shown in Fig. 6A. This resulted in a final DV value of 1.5 L water/L feed for the 1 kDa diafiltration in *Cycle A*, 4.9 L water/L feed for the 10 kDa diafiltration in *Cycle B,* and 0.4 L water/L feed for the 1 kDa diafiltration in *Cycle B*. The fractionation and purification results at the end of each filtration stage for both fractionation cascades are shown in Fig. 6B and Table 4.

3.4.1. *Results for Cycle A: purity degree and fractionation yield*

In *Cycle A* (Fig. 2), OSH was diafiltered through a 100 kDa membrane, and then the first permeate p1 from the 100 kDa membrane was subjected to a diafiltration through a 1 kDa membrane. As can be observed in Fig. 6B and in Table S2, a successful removal (>97 %) of the different monomeric compounds was achieved, which were collected in the final permeate pA. Thus, even the 1 kDa membrane scarcely retained free monosaccharides, organic acids, furfural and phenolic compounds. However, these membranes effectively retained a substantial portion of the onion skin POS, approximately 90.1 %, with around 33.7 % recovered in the first retentate r1 from the 100 kDa membrane and followed by about 56.5 % recovered in the second retentate rA from the 1 kDa membrane.

The comparison of the POS molecular weight distribution (Table 4) and recovery factors (RF_{POS}) for the permeate and retentate from the

100 kDa membrane shows that the retentate r1 turned out to be a product enriched in POS species above 80 kDa (peak 1, ~90.3 % of the total area in r1) with low content in the other POS species (peaks 2–5), which were collected in the permeate p1 (peaks 2–5, ~70 % of total area in p1). Furthermore, the permeate p1 exhibited a first peak of POS species ranging from approximately 80 to 30 kDa (peak 1 in p1, with average molecular weight value close to 42 kDa), constituting around 29 % of the total area. These results suggest that the 100 kDa membrane was enough to obtain complete retention of the POS species with a molecular weight above 80 kDa, which was found to be approximately 30 % of the initial oligosaccharides in the onion skin hydrolysate.

In the second diafiltration stage, it can be inferred from the results of GPC analysis and recovery factor that even the smallest POS species present in the permeate p1 (feed) were mostly recovered in the retentate rA from the 1 kDa membrane. This is evidenced by the similar retention factor in both streams and by the detection of all POS species (peaks 1–5) found in the permeate p1 also in the retentate rA, as well as similar relative proportions of the different POS fractions.

Finally, it can also be seen from Table 4 that the onion skin POS recovered in these final retentates (r1 and rA) exhibited high purity, and a significantly narrower molecular weight range compared to the total POS in the initial OSH. The first retentate r1 from the 100 kDa membrane has been identified as a POS product enriched in less hydrolysed POS species from the initial OSH, with an average molecular weight close to 79 kDa, and a greater value of the degree of branching (RG-I = 36.1 %) compared to the total POS in the OSH (RG-I = 28.5 %). In contrast, the retentate rA from the 1 kDa membrane was composed by all POS fractions below 80 kDa, accounting for 56 % of the initial POS in the OSH. This POS product showed an average molecular weight of about 20 kDa and a degree of branching similar to the total POS in the OSH (RG-I = 27 % and 28.5 % for POS in rA and in OSH respectively). Consequently, it can be concluded that this sequential diafiltration process has been effective in yielding two valuable high-purity fractions of POS with a narrower molecular weight distribution than the OSH, along with low molecular weight molecules collected in the final permeate.

3.4.2. Results for Cycle B: fractionation efficiency of onion skin pectic oligosaccharides

In the second cycle (*Cycle B*, Fig. 2), the permeate p1 from the 100 kDa membrane was filtered in concentration mode with a 10 kDa membrane, and then, the permeate and retentate of this concentration stage were diafiltrated with a 1 and 10 kDa membrane, respectively. This proposed sequence aims to further study the fractionation of POS species present in the permeate p1. As shown in Fig. 6B, most of the total POS content (87 %) was recovered in the final retentate streams. Specifically, 33.7 %, 29.3 %, and 24.1 % were distributed in the retentate r1 from the 100 kDa membrane, in the retentate rB1 from the 10 kDa membrane, and in the retentate rB2 from the 1 kDa membrane, respectively. It should be noted that the results for the retentate r1 were statistically similar in both fractionation cycles.

The comparison of recovery factors (RF_{POS}) and the molecular weight distribution (Table 4) confirmed the fractionation of the POS species present in the OSH in three products with noticeable differences in terms of molecular weight range. It was observed that the average molecular weight differed notably among the three POS products, with values close to 79, 36 and 7 kDa for the retentate r1, rB1, and rB2, respectively. The retentate r1 turned out to be a POS product enriched in less hydrolysed POS above 80 kDa, the retentate rB1 was primarily composed for the POS species from 20 to 80 kDa (peaks 1 and 2, ~88.4 % of the total area), and finally, the retentate rB2 can be considered as a product enriched in POS species below 20 kDa (peaks 3–5, ~98.6 % of the total area). In addition, significant differences were also observed in the extent of branching, which decreased as the average molecular weight of the POS products decreased. Nevertheless, the degree of branching for all POS products remained over 20 %, indicating that even the more hydrolysed POS species preserved a considerable portion of the onion skin pectin RG-I branches.

With regard to purity (Figs. 6B), 87 % of total monosaccharides, organic acids, and sugar dehydration products, along with 91 % of total phenolic compounds (Table S3), were collected in the final permeate pB. In any case, an increase of the final VD for diafiltration with the 1 kDa membrane will result in a higher recovery of low-molecular-weight compounds in the pB permeate, since the low retention of the 1 kDa membrane towards these monomeric compounds has already been demonstrated previously.

In summary, the combination of diafiltration and cascade operation has yielded various types of onion skin pectic oligosaccharide (POS) products, demonstrating their potential for diverse applications owing to their high purity, significant degree of branching, and narrow molecular weight range. However, it is important to note that further research is necessary to assess the distinct functional properties of the fractionated oligosaccharides obtained in *Cycle A* and *Cycle B* of this work.

4. Conclusions

Onion skin waste recovered after quercetin extraction was an excellent source of natural pectin, from which pectic oligosaccharides have been produced using an integrated process of subcritical water extraction followed by diafiltration purification. The subcritical water hydrolysate from this solid residue was found to be a complex multicomponent mixture with a large variety of pectic oligosaccharides of different molecular weight. Experiments conducted in total recirculation mode yielded valuable results regarding the effect of transmembrane pressure and the membrane cutoff size on permeate flux and separation capacity. The reduction of the membrane molecular weight cutoff from 100 kDa to 1 kDa favoured the retention of pectic oligosaccharides, confirming the potential of membrane separation processes for its fractionation. A comparison of membrane retention with the molecular size distribution of pectic oligosaccharides revealed complete retention of the largest pectic oligosaccharides with all membranes (100, 50, 10 and 1 kDa), good retention of the intermediate pectic oligosaccharides ranging from 10 to 30 kDa with the 1 kDa and 10 kDa membranes, while the smallest oligosaccharides below 10 kDa were exclusively retained by the 1 kDa membrane. Additionally, all ultrafiltration membranes exhibited high selectivity for separating pectic oligosaccharides from other compounds present in the onion skin hydrolysate, thus justifying the potential to achieve high purification yields. For the separation of the less hydrolysed onion skin pectic oligosaccharides, no significant differences in terms of oligosaccharide fractionation were found using the 50 kDa and 100 kDa membranes. Nevertheless, the results of the onion skin hydrolysate diafiltration across the 50 and 100 kDa membranes have provided information on the water consumption required to achieve similar oligosaccharide purification, which significantly increased with the 50 kDa membrane due to irreversible fouling effects.

The combination of diafiltration and cascade operation, using sequential diafiltration stages with 100, 10, and 1 kDa membranes, has enabled the fractionation and purification of the total pectic oligosaccharides present in the onion skin subcritical water hydrolysate. The diafiltration mass balance applied to different compounds of the hydrolysate allowed a suitable prediction of fractionation and purification of oligosaccharides throughout the diafiltration process. Approximately 87 wt% of the initial oligosaccharides were successfully recovered and purified in the different retentates. Specifically, 33.7 %, 29.3 %, and 24.1 % were recovered in the retentate from the 100, 10, and 1 kDa membranes, respectively. The average molecular weight differed notably among the three pectic oligosaccharide fractions (79, 36 and 7 kDa), with no significant variation in the degree of branching, which remained over 20 % for all products. This highlights the feasibility of the integrated subcritical water/diafiltration process for obtaining diverse high-purity products of onion skin pectic oligosaccharides with distinct

range of molecular weights and significant branching, offering an improvement for further industrial exploitation.

CRediT authorship contribution statement

M.O. Ruiz: Writing – review & editing, Writing – original draft, Visualization, Validation, Methodology, Investigation, Formal analysis, Data curation, Conceptualization. **Ó. Benito-Román:** Writing – review & editing, Writing – original draft, Validation, Supervision, Project administration, Methodology, Investigation, Funding acquisition, Formal analysis, Conceptualization. **S. Beltrán:** Writing – review & editing, Supervision, Project administration, Methodology, Investigation, Funding acquisition, Conceptualization. **M.T. Sanz:** Writing – review & editing, Supervision, Project administration, Methodology, Investigation, Funding acquisition, Conceptualization.

Declaration of competing interest

The authors declare that they have no known competing financial interests or personal relationships that could have appeared to influence the work reported in this paper.

Data availability

The experimental data from this research are included in the manuscript

Acknowledgments

This work was supported by the Agencia Estatal de Investigación [grant numbers PID2020-116716RJ-I00, PDC2022-133443-I00, PID2022-136385OB-I00] and the Junta de Castilla y León (JCyL) and the European Regional Development Fund (ERDF) [grant number BU027P23]. Benito Román post-doctoral contract was funded by the Agencia Estatal de Investigación through project PID2020–116716RJ-I00.

Appendix A. Supplementary data

Supplementary data to this article can be found online at https://doi.org/10.1016/j.memsci.2024.123054.

Nomenclature

List of symbols

A	membrane area (m^2)
AcA	acetic acid
ara	arabinose
C	compound concentration (mg L^{-1})
CFD	continuous feed diafiltration
CFV	crossflow velocity (m s^{-1})
DV	diafiltration volume
F	furfural
FA	Formic acid
GA	free galacturonic acid
gal	galactose
GAO	galacturonic acid oligomers
glu	glucose
HMF	hydroxymethyl furfural
IOSR	industrial onion skin residues
J	permeate flux (L $m^{-2}{\cdot}h^{-1}$)
J*	critical flux parameter defined in Eq. (5) (L $m^{-2}{\cdot}h^{-1}$)
J_0	pure water permeate flux (L $m^{-2}{\cdot}h^{-1}$)
k	parameter of Eqs. (4) and (12)
k_c	fouling index of Eqs. (7) and (15) (s^{-1})
k_{cl}	fouling index of Eqs. (5) and (13) (s m^{-2})
k_s	fouling index of Eqs. (6) and (14) ($s^{-0.5}m^{-0.5}$)
MS	total free monosaccharides
MW	molecular weight
MWCO	molecular weight cutoff of the ultrafiltration membranes
n	parameter of Eqs. (4) and (12)
OA	total organic acids
OSH	onion skin hydrolysate
POS	pectic oligosaccharides
r_f	fouling resistance of Eq. (3) (m^{-1})
r_m	membrane hydraulic resistance of Eq. (3) (m^{-1})
r_T	total resistance to filtration of Eq. (3) (m^{-1})
R	retention coefficient defined in Eq. 8
RF	retention factor (wt.%)
R^2	determination coefficient
rha	rhamnose
SubW	subcritical water

T	transmission coefficient defined in Eq. 9
TMP	transmembrane pressure
TPC	total phenolic compounds
V	volume (L)
VRF	volume reduction factor
xyl	xylose

Greek symbols

α	selectivity defined in Eq. 10
ξ	zeta potential
ρ	density (kg/m^3)
μ	viscosity of the permeate (Pa·s)

Subscripts

F	onion hydrolysate used as feed solution
i	hydrolysate compound
j	each group of hydrolysate compounds, without the oligosaccharide fraction
p	permeate stream
r	retentate stream
w	pure water for the continuous feed diafiltration experiments

References

[1] V. Benítez, E. Mollá, M.A. Martín-Cabrejas, Y. Aguilera, F.J. López-Andréu, K. Cools, L.A. Terry, R.M. Esteban, Characterization of industrial onion wastes (Allium cepa L.): dietary fibre and bioactive compounds, Plant Foods Hum. Nutr. 66 (2011) 48–57, https://doi.org/10.1007/s11130-011-0212-x.

[2] Ó. Benito-Román, B. Blanco, M.T. Sanz, S. Beltrán, Subcritical water extraction of phenolic compounds from onion skin wastes (*Allium cepa cv. Horcal*): effect of temperature and solvent properties, Antioxidants 9 (2020) 1–20, https://doi.org/10.3390/antiox9121233.

[3] I.S. Choi, E.J. Cho, J.H. Moon, H.J. Bae, Onion skin waste as a valorization resource for the by-products quercetin and biosugar, Food Chem. 188 (2015) 537–542, https://doi.org/10.1016/j.foodchem.2015.05.028.

[4] L.R. Adetunji, A. Adekunle, V. Orsat, V. Raghavan, Advances in the pectin production process using novel extraction techniques: a review, Food Hydrocolloids 62 (2017) 239–250, https://doi.org/10.1016/j.foodhyd.2016.08.015.

[5] N. Babbar, W. Dejonghe, M. Gatti, S. Sforza, K. Elst, Pectic oligosaccharides from agricultural by-products: production, characterization and health benefits, Crit. Rev. Biotechnol. 36 (2016) 594–606, https://doi.org/10.3109/07388551.2014.996732.

[6] L.N. Gerschenson, The production of galacturonic acid enriched fractions and their functionality, Food Hydrocolloids 68 (2017) 23–30, https://doi.org/10.1016/j.foodhyd.2016.11.030.

[7] Z.K. Muhidinov, K.I. Ikromi, A.S. Jonmurodov, A.S. Nasriddinov, S.R. Usmanova, J. T. Bobokalonov, G.D. Strahan, L.S. Liu, Structural characterization of pectin obtained by different purification methods, Int. J. Biol. Macromol. 183 (2021) 2227–2237, https://doi.org/10.1016/j.ijbiomac.2021.05.094.

[8] P. Alonso-Riaño, C. Ramos, E. Trigueros, S. Beltrán, M.T. Sanz, Study of subcritical water scale-up from laboratory to pilot system for brewer's spent grain valorization, Ind. Crops Prod. 191 (2023) 1–13, https://doi.org/10.1016/j.indcrop.2022.115927.

[9] P. Barea, R. Melgosa, A.E. Illera, P. Alonso-Riaño, E. Díaz de Cerio, O. Benito-Román, S. Beltrán, M.T. Sanz, Production of small peptides and low molecular weight amino acids by subcritical water from fish meal: effect of pressurization agent, Food Chem. 418 (2023), https://doi.org/10.1016/j.foodchem.2023.135925.

[10] F.P. Cardenas-Toro, T. Forster-Carneiro, M.A. Rostagno, A.J. Petenate, F. Maugeri Filho, M.A.A. Meireles, Integrated supercritical fluid extraction and subcritical water hydrolysis for the recovery of bioactive compounds from pressed palm fiber, J. Supercrit. Fluids 93 (2014) 42–48, https://doi.org/10.1016/j.supflu.2014.02.009.

[11] E. Trigueros, C. Ramos, P. Alonso-Riaño, S. Beltrán, M.T. Sanz, Subcritical water treatment for valorization of the red algae residue after agar extraction: scale-up from laboratory to pilot plant, Ind. Eng. Chem. Res. 62 (2023) 3503–3514, https://doi.org/10.1021/acs.iecr.2c04132.

[12] S.Q. Liew, W.H. Teoh, R. Yusoff, G.C. Ngoh, Comparisons of process intensifying methods in the extraction of pectin from pomelo peel, Chem. Eng. Process. - Process Intensif. 143 (2019) 107586, https://doi.org/10.1016/j.cep.2019.107586.

[13] M. Plaza, C. Turner, Pressurized hot water extraction of bioactives, TrAC, Trends Anal. Chem. 71 (2015) 39–54, https://doi.org/10.1016/j.trac.2015.02.022.

[14] O. Benito-Román, P. Alonso-Riaño, E. Díaz De Cerio, M.T. Sanz, S. Beltrán, Semi-continuous hydrolysis of onion skin wastes with subcritical water: pectin recovery and oligomers identification, J. Environ. Chem. Eng. 10 (2022) 107439, https://doi.org/10.1016/j.jece.2022.107439.

[15] B. Gómez, B. Gullón, R. Yáñez, J.C. Parajó, J.L. Alonso, Pectic oligosacharides from lemon peel wastes: production, purification, and chemical characterization, J. Agric. Food Chem. 61 (2013) 10043–10053, https://doi.org/10.1021/jf402559p.

[16] L. Jin, F. Zuo, Y. Gao, S. Sui, D. Zhang, Purification of pectin by ultrafiltration in combination with sodium citrate, J. Food Eng. 335 (2022) 111158, https://doi.org/10.1016/j.jfoodeng.2022.111158.

[17] M. Ramos-Andres, B. Aguilera-Torre, J. García-Serna, Production of purified hemicellulose-pectin fractions of different molecular weight from discarded carrots by hydrothermal treatment followed by multistep ultrafiltration/diafiltration, J. Clean. Prod. 321 (2021) 128923, https://doi.org/10.1016/j.jclepro.2021.128923.

[18] F. Dranca, M. Oroian, Extraction, purification and characterization of pectin from alternative sources with potential technological applications, Food Res. Int. 113 (2018) 327–350, https://doi.org/10.1016/j.foodres.2018.06.065.

[19] B.M. Yapo, B. Wathelet, M. Paquot, Comparison of alcohol precipitation and membrane filtration effects on sugar beet pulp pectin chemical features and surface properties, Food Hydrocolloids 21 (2007) 245–255, https://doi.org/10.1016/j.foodhyd.2006.03.016.

[20] N. Muñoz-Almagro, M. Prodanov, P.J. Wilde, M. Villamiel, A. Montilla, Obtainment and characterisation of pectin from sunflower heads purified by membrane separation techniques, Food Chem. 318 (2020) 126476, https://doi.org/10.1016/j.foodchem.2020.126476.

[21] M. Ramos-Andrés, S. Díaz-Cesteros, N. Majithia, J. García-Serna, Pilot-scale biorefinery for the production of purified biopolymers based on hydrothermal treatment in flow-through reactor cycles, Chem. Eng. J. 437 (2022) 135123, https://doi.org/10.1016/j.cej.2022.135123.

[22] R. Paulen, M. Fikar, G. Foley, Z. Kovács, P. Czermak, Optimal feeding strategy of diafiltration buffer in batch membrane processes, J. Membr. Sci. 411–412 (2012) 160–172, https://doi.org/10.1016/j.memsci.2012.04.028.

[23] N. Oueslati, P. Leblanc, A. Bodin, C. Harscoat-Schiavo, E. Rondags, S. Meunier, I. Marc, R. Kapel, A simple methodology for predicting the performances of hyaluronic acid purification by diafiltration, J. Membr. Sci. 490 (2015) 152–159, https://doi.org/10.1016/j.memsci.2015.04.024.

[24] T. Qi, X. Da, Y. Zhang, X. Chen, Z. Cui, M. Qiu, Y. Fan, Modeling and optimal operation of intermittent feed diafiltration for refining oligodextran using nanoporous ceramic membranes, Sep. Purif. Technol. 253 (2020) 117491, https://doi.org/10.1016/j.seppur.2020.117491.

[25] S. Yammine, R. Rabagliato, X. Vitrac, M.M. Peuchot, R. Ghidossi, Selecting ultrafiltration membranes for fractionation of high added value compounds from grape pomace extracts, Oeno One 53 (2019) 487–497, https://doi.org/10.20870/oeno-one.2019.53.3.2343.

[26] M. Pinelo, G. Jonsson, A.S. Meyer, Membrane technology for purification of enzymatically produced oligosaccharides: molecular and operational features affecting performance, Sep. Purif. Technol. 70 (2009) 1–11, https://doi.org/10.1016/j.seppur.2009.08.010.

[27] T. Qi, X. Chen, W. Shi, T. Wang, M. Qiu, X. Da, J. Wen, Y. Fan, Fouling behavior of nanoporous ceramic membranes in the filtration of oligosaccharides at different temperatures, Sep. Purif. Technol. 278 (2022) 119589, https://doi.org/10.1016/j.seppur.2021.119589.

[28] Y.S. Lin, Inorganic membranes for process intensification: challenges and perspective, Ind. Eng. Chem. Res. 58 (2019) 5787–5796, https://doi.org/10.1021/acs.iecr.8b04539.

[29] A. Echavarria, J. Pagán, A. Ibarz, Effect of previous enzymatic recirculation treatment through a tubular ceramic membrane on ultrafiltration of model solution and apple juice, J. Food Eng. 102 (2011) 334–339, https://doi.org/10.1016/j.jfoodeng.2010.09.009.

[30] E. Trigueros, M.T. Sanz, S. Beltrán, M.O. Ruiz, Filtration of subcritical water hydrolysates from red macroalgae byproducts with ultraporous ceramic membranes for oligosaccharide and peptide fractionation, J. Membr. Sci. 660 (2022) 120822, https://doi.org/10.1016/j.memsci.2022.120822.
[31] M. Moresi, I. Sebastiani, Pectin recovery from model solutions using a laboratory-scale ceramic tubular UF membrane module, J. Membr. Sci. 322 (2008) 349–359, https://doi.org/10.1016/j.memsci.2008.05.066.
[32] C. Saf, M. Villain-Gambier, M. Belaqziz, I. Ziegler-Devin, D. Trebouet, N. Ouazzani, Fouling control investigation by pH optimization during olive mill wastewater ultrafiltration, Process Saf. Environ. Protect. 164 (2022) 119–128, https://doi.org/10.1016/j.psep.2022.06.010.
[33] G.T. Vladisavljević, P. Vukosavljević, M.S. Veljović, Clarification of red raspberry juice using microfiltration with gas backwashing: a viable strategy to maximize permeate flux and minimize a loss of anthocyanins, Food Bioprod. Process. 91 (2013) 473–480, https://doi.org/10.1016/j.fbp.2013.05.004.
[34] T. Moritz, S. Benfer, P. Árki, G. Tomandl, Influence of the surface charge on the permeate flux in the dead-end filtration with ceramic membranes, Sep. Purif. Technol. 25 (2001) 501–508, https://doi.org/10.1016/S1383-5866(01)00080-6.
[35] N.H. M'sakni, H. Majdoub, S. Roudesli, L. Picton, D. Le Cerf, C. Rihouey, C. Morvan, Composition, structure and solution properties of polysaccharides extracted from leaves of Mesembryanthenum crystallinum, Eur. Polym. J. 42 (2006) 786–795, https://doi.org/10.1016/j.eurpolymj.2005.09.014.
[36] M. Kaszuba, J. Corbett, F.M.N. Watson, A. Jones, High-concentration zeta potential measurements using light-scattering techniques, Philos. Trans. R. Soc. A Math. Phys. Eng. Sci. 368 (2010) 4439–4451, https://doi.org/10.1098/rsta.2010.0175.
[37] J. Hermia, Constant pressure blocking filtration laws - application to power-law non-Newtonian fluids, Inst. Chem. Eng. Trans. 60 (1982) 183–187.
[38] R.W. Field, D. Wu, J.A. Howell, B.B. Gupta, Critical flux concept for microfiltration fouling, J. Membr. Sci. 100 (1995) 259–272, https://doi.org/10.1016/0376-7388(94)00265-Z.
[39] M.C. Vincent Vela, S. Álvarez Blanco, J. Lora García, E. Bergantiños Rodríguez, Analysis of membrane pore blocking models adapted to crossflow ultrafiltration in the ultrafiltration of PEG, Chem. Eng. J. 149 (2009) 232–241, https://doi.org/10.1016/j.cej.2008.10.027.
[40] H. Pińkowska, M. Krzywonos, P. Wolak, A. Złocińska, Production of uronic acids by hydrothermolysis of pectin as a model substance for plant biomass waste, Green Process. Synth. 8 (1) (2019) 683–690, https://doi.org/10.1515/gps-2019-0039.
[41] M. Martínez, R. Yáñez, J.L. Alonsó, J.C. Parajó, Chemical production of pectic oligosaccharides from orange peel wastes, Ind. Eng. Chem. Res. 49 (2010) 8470–8476, https://doi.org/10.1021/ie101066m.
[42] Y. Neggaz, M.L. Vargas, A.O. Dris, F. Riera, R. Alvarez, A combination of serial resistances and concentration polarization models along the membrane in ultrafiltration of pectin and albumin solutions, Sep. Purif. Technol. 54 (2007) 18–27, https://doi.org/10.1016/j.seppur.2006.08.017.
[43] M.Z. Sulaiman, N.M. Sulaiman, M. Shamel, Ultrafiltration studies on solutions of pectin, glucose and their mixtures in a pilot scale crossflow membrane unit, Chem. Eng. J. 84 (2001) 557–563, https://doi.org/10.1016/S1385-8947(01)00133-4.
[44] P. Bacchin, P. Aimar, R.W. Field, Critical and sustainable fluxes: theory, experiments and applications, J. Membr. Sci. 281 (2006) 42–69, https://doi.org/10.1016/j.memsci.2006.04.014.
[45] G. Mao, D. Wu, C. Wei, W. Tao, X. Ye, R.J. Linhardt, C. Orfila, S. Chen, Reconsidering conventional and innovative methods for pectin extraction from fruit and vegetable waste: targeting rhamnogalacturonan I, Trends Food Sci. Technol. 94 (2019) 65–78, https://doi.org/10.1016/j.tifs.2019.11.001.
[46] M.I. Jiménez-Maldonado, M.E. Tiznado-Hernández, A. Rascón-Chu, E. Carvajal-Millán, J. Lizardi-Mendoza, R. Troncoso-Rojas, Analysis of rhamnogalacturonan I fragments as elicitors of the defense mechanism in tomato fruit, Chil. J. Agric. Res. 78 (2018) 339–349, https://doi.org/10.4067/S0718-58392018000300339.
[47] H. Shi, L. Yu, Y. Shi, J. Lu, H. Teng, Y. Zhou, L. Sun, Structural characterization of a rhamnogalacturonan I domain from ginseng and its inhibitory effect on galectin-3, Molecules 22 (2017) 11–14, https://doi.org/10.3390/molecules22061016.
[48] X. Meng, D. Luosang, S. Meng, R. Wang, W. Fan, D. Liang, X. Li, Q. Zhao, L. Yang, The structural and functional properties of polysaccharide foulants in membrane fouling, Chemosphere 268 (2021) 129364, https://doi.org/10.1016/j.chemosphere.2020.129364.
[49] M.L. Gimenes, V.R. Silva, F. Hamerski, A.P. Scheer, Pretreatment of aqueous pectin solution by cross-flow microfiltration: study on fouling mechanism, Int. J. Chem. Eng. Appl. 5 (3) (2014) 281–286, https://doi.org/10.7763/ijcea.2014.v5.394.
[50] L. Xie, X. Li, Y. Guo, Ultrafiltration behaviors of pectin-containing solution extracted from citrus peel on a ZrO_2 ceramic membrane pilot unit, Korean, J. Chem. Eng. 25 (1) (2008) 149–153, https://doi.org/10.1007/s11814-008-0027-0.
[51] P. Rai, G.C. Majumdar, S. Dasgupta, S. De, Understanding ultrafiltration performance with mosambi juice in an unstirred batchcell, J. Food Process. Eng. 28 (2005) 166–180, https://doi.org/10.1111/j.1745-4530.2005.00399.x.
[52] B. Sarkar, A combined complete pore blocking and cake filtration model during ultrafiltration of polysaccharide in a batch cell, J. Food Eng. 116 (2) (2013) 333–343, https://doi.org/10.1016/j.jfoodeng.2012.12.013.
[53] D.T.N.N. Nguyen, M.L. Lameloise, W. Guiga, R. Lewandowski, M. Bouix, C. Fargues, Optimization and modeling of diananofiltration process for the detoxification of lingo-cellulosic hydrolysates – study at pre-industrial scale, J. Membr. Sci. 512 (2016) 111–121, https://doi.org/10.1016/j.memsci.2016.04.008.
[54] C.W. Cho, D.Y. Lee, C.W. Kim, Concentration and purification of soluble pectin from Mandarin peels using crossflow microfiltration system, Carbohydr. Polym. 54 (2003) 21–26, https://doi.org/10.1016/S0144-8617(03)00133-4.
[55] P. Alonso-Vázquez, C. Valle, C. Sánchez-Arévalo, B.-E. Cuartas-Uribe, M.-C. Vincent-Vela, A. Bes-Piá, S. Álvarez-Blanco, Separation of phenolic compounds from canned Mandarin production wastewater by ultrafiltration and nanofiltration, J. Water Process Eng. 59 (2024) 105041, https://doi.org/10.1016/j.jwpe.2024.105041.
[56] A. Cassano, C. Conidi, L. Giorno, E. Drioli, Fractionation of olive mill wastewaters by membrane separation technique, J. Hazard Mater. 248–249 (2013) 185–193, https://doi.org/10.1016/j.jhazmat.2013.01.006.
[57] A. Giacobbo, A.M. Bernardes, M. Norberta de Pinho, Sequential pressure-driven membrane operations to recover and fractionate polyphenols and polysaccharides from second racking wine lees, Sep. Purif. Technol. 173 (2017) 49–54, https://doi.org/10.1016/j.seppur.2016.09.007.
[58] A. Servent, F.A.P. Abreu, C. Dhuique-mayer, M. Belleville, M. Dornier, Concentration and purification by crossflow microfiltration with diafiltration of carotenoids from a by-product of cashew apple juice processing, Innovat. Food Sci. Emerg. Technol. 66 (2020) 102519, https://doi.org/10.1016/j.ifset.2020.102519.